Turbulent Reconnection of Magnetic Bipoles in Stratified Turbulence

I. ROGACHEVSKII, N. KLEEORIN,

Ben-Gurion University of the Negev, Beer Sheva, Israel

NORDITA, KTH Royal Institute of Technology and Stockholm University, Sweden

A. BRANDENBURG, S. JABBARI, Dh. MITRA

NORDITA, KTH Royal Institute of Technology and Stockholm University, and Department of Astronomy, Stockholm University, Sweden

Thanks to A. Schekochihin (Oxford)

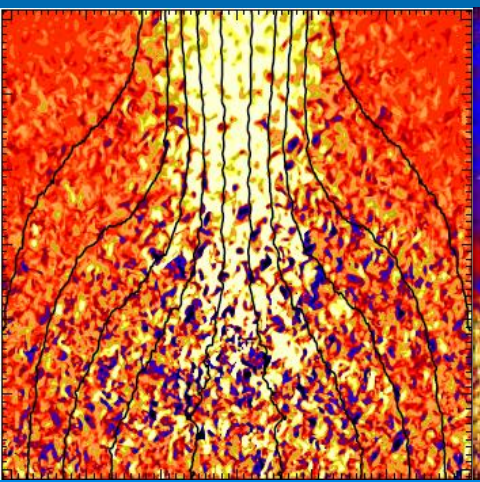

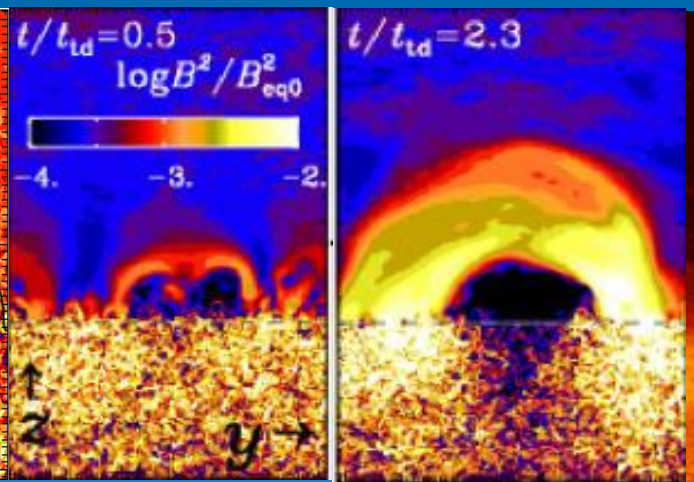

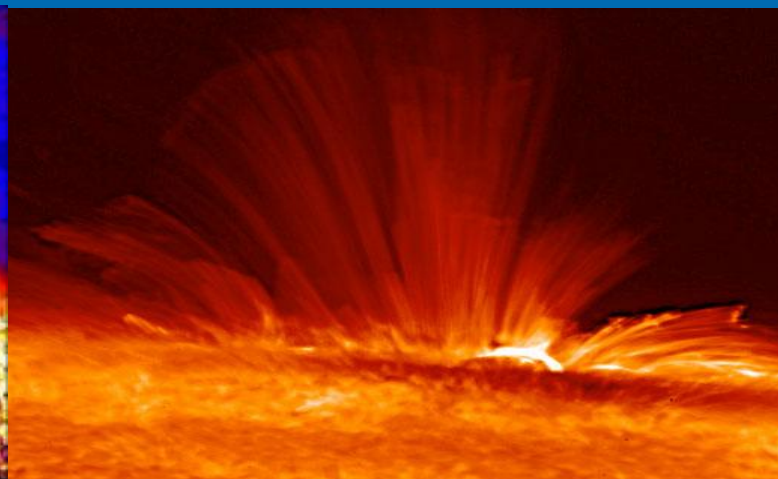

Mean-Field Dynamo

Mean-Field Approach: $B = \overline{B} + b,$ $U = \overline{U} + u,$

- **Induction equation for mean magnetic field:**

$$\frac{\partial \overline{B}}{\partial t} = \nabla \times \left(\overline{U} \times \overline{B} + \langle u \times b \rangle \right) + \eta \Delta \overline{B},$$

$\overline{B} = \langle B \rangle$

$\overline{U} = \langle U \rangle$

- **Turbulent electromotive force:**

$\mathcal{E} = \langle u \times b \rangle,$

$$\mathcal{E} = \alpha \overline{B} + V^{\text{eff}} \times \overline{B} - \eta_T (\nabla \times \overline{B}),$$

$\eta_T = \frac{\tau_0}{3} \langle u^2 \rangle.$

$V^{\text{eff}} = -\frac{1}{2} \nabla \eta_T.$

$\alpha = -\frac{\tau_0}{3} \langle u \cdot (\nabla \times u) \rangle.$

Steenbeck, Krause, Rädler (1966)

Alpha Effect

$$\alpha = -\frac{\tau_0}{3} \langle \boldsymbol{u} \cdot (\boldsymbol{\nabla} \times \boldsymbol{u}) \rangle .$$

I. Rogachevskii* and N. Kleeorin

MNRAS **547,** 1–13 (2026)

$$\alpha^{(\lambda)} = \frac{13}{45} \ell_0^2 \, (\boldsymbol{\lambda} \cdot \overline{\boldsymbol{W}}) .$$

$$\boldsymbol{\lambda} = -(\boldsymbol{\nabla} \overline{\rho}) / \overline{\rho}.$$

$$\overline{\boldsymbol{W}} = \boldsymbol{\nabla} \times \overline{\boldsymbol{U}}$$

$$\alpha^{(\Lambda)} = -\frac{\ell_0^2}{9} \, (\boldsymbol{\Lambda} \cdot \overline{\boldsymbol{W}})$$

$$\boldsymbol{\Lambda} = \boldsymbol{\nabla} \ln \langle \boldsymbol{u}^2 \rangle^{(0)}.$$

$$\alpha^{(\Omega)} \propto -\ell_0^2 \left(\overline{\boldsymbol{\Omega}} \cdot \boldsymbol{\nabla} \right) \ln \left(\overline{\rho}^{\, \mu_*} \, u_{\rm rms} \right),$$

The α^2 Dynamo

$$\frac{\partial \overline{B}}{\partial t} = \nabla \times \left(\alpha \overline{B} - \eta_{\mathrm{T}} \nabla \times \overline{B} \right),$$

$$\overline{B}(t, X, Z) = \overline{B}_y(t, X, Z) \boldsymbol{e}_y + \nabla \times \left[\overline{A}(t, X, Z) \boldsymbol{e}_y \right],$$

$$\gamma = |\alpha K| - \eta_{\mathrm{T}} K^2,$$

$$K^{\max} = |\alpha| / 2\eta_{\mathrm{T}}$$

$$\gamma^{\max} = \alpha^2 / 4\eta_{\mathrm{T}}.$$

Nonlinear Effect: Magnetic Part of Alpha effect

- Induction equation for **mean magnetic field**:

$$\frac{\partial \overline{B}}{\partial t} = \nabla \times \left(\alpha \overline{B} - \eta_T \nabla \times \overline{B} \right),$$

- **Electromotive force**:

$$\boldsymbol{\varepsilon} \equiv \langle \mathbf{u} \times \mathbf{b} \rangle = \alpha \mathbf{B} - \eta_T \nabla \times \mathbf{B} + \ldots$$

$$\alpha = -\frac{\tau}{3} \langle \mathbf{u} \cdot \mathbf{rot}\, \mathbf{u} \rangle + \frac{\tau}{12\pi\rho} \underbrace{\langle \mathbf{b} \cdot \mathbf{rot}\, \mathbf{b} \rangle}_{\sim \mathbf{a} \cdot \mathbf{b}}$$

A. Pouquet, U. Frisch, and J. Leorat, J. Fluid Mech. 77, 321 (1976)

Magnetic Helicity

Total magnetic helicity is conserved for very large magnetic Reynolds numbers

$$\chi^m_{\text{total}}(\mathbf{B}) = \mathbf{A}\cdot\mathbf{B} + \langle \mathbf{a}\cdot\mathbf{b}\rangle \to const$$

Magnetic part of alpha effect:

$$\alpha^m = \chi^c(\mathbf{B})\,\Phi_m(B)$$

The dynamic nonlinearity:

$$\chi^c(\mathbf{B}) \sim \frac{2}{9\eta_T\rho}\langle \mathbf{a}\cdot\mathbf{b}\rangle$$

The evolutionary equation: $\chi^{(m)}(\mathbf{B}) = \langle \mathbf{a}\cdot\mathbf{b}\rangle$

Problems

- What is the mechanism of formation of magnetic structures in turbulence?
- Dynamo mechanism can generate only weak (<< 1000G) nearly uniform large-scale magnetic field.
- How is it possible to create strongly inhomogeneous magnetic structures from originally uniform magnetic field?

Active regions and Sunspots

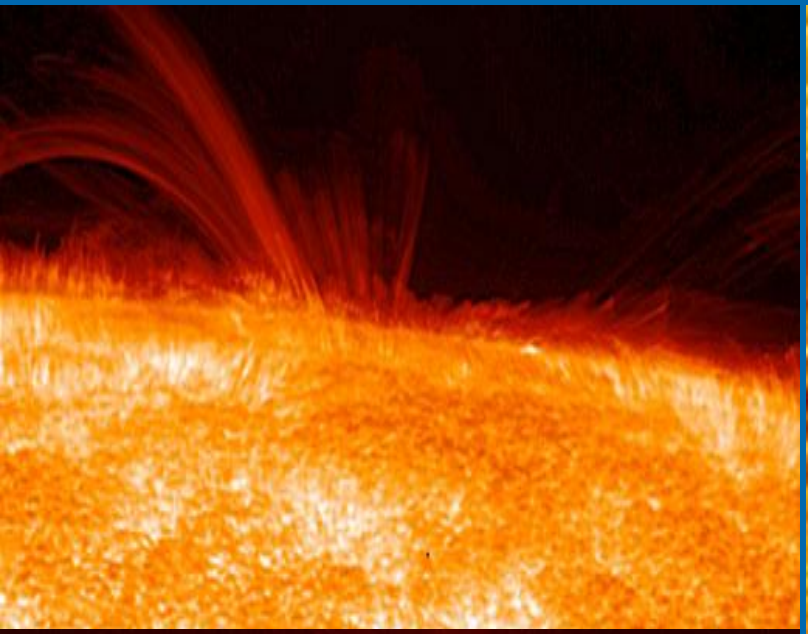

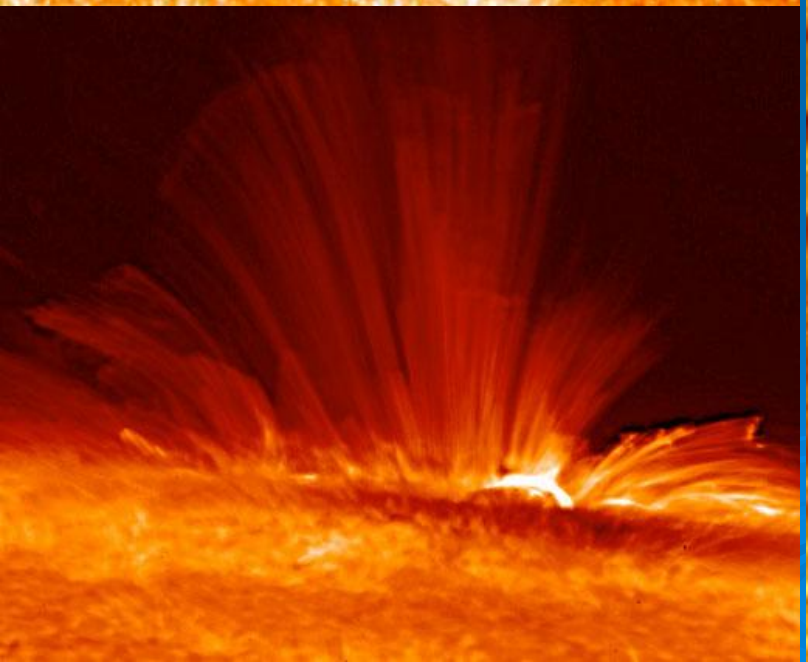

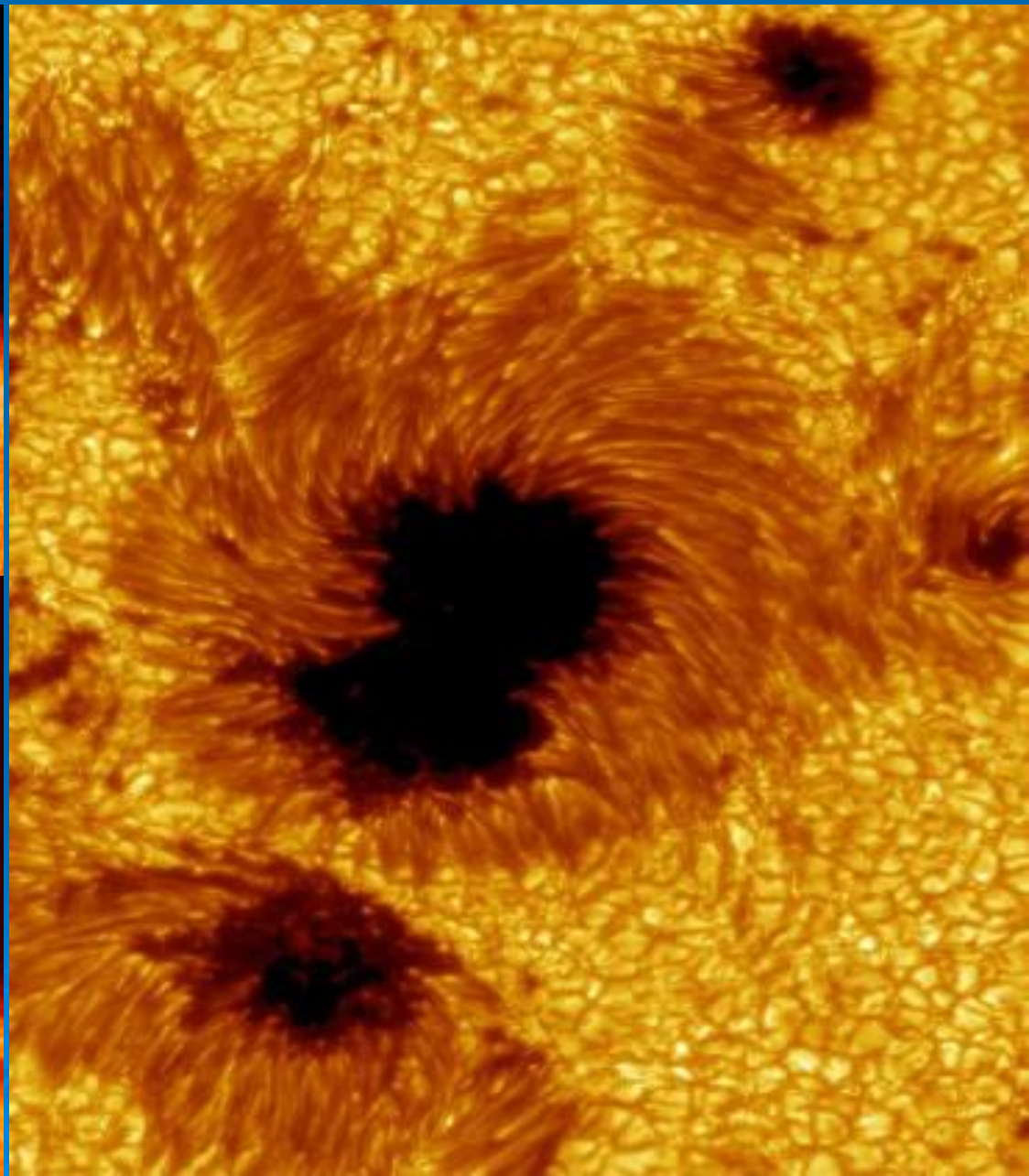

Active regions

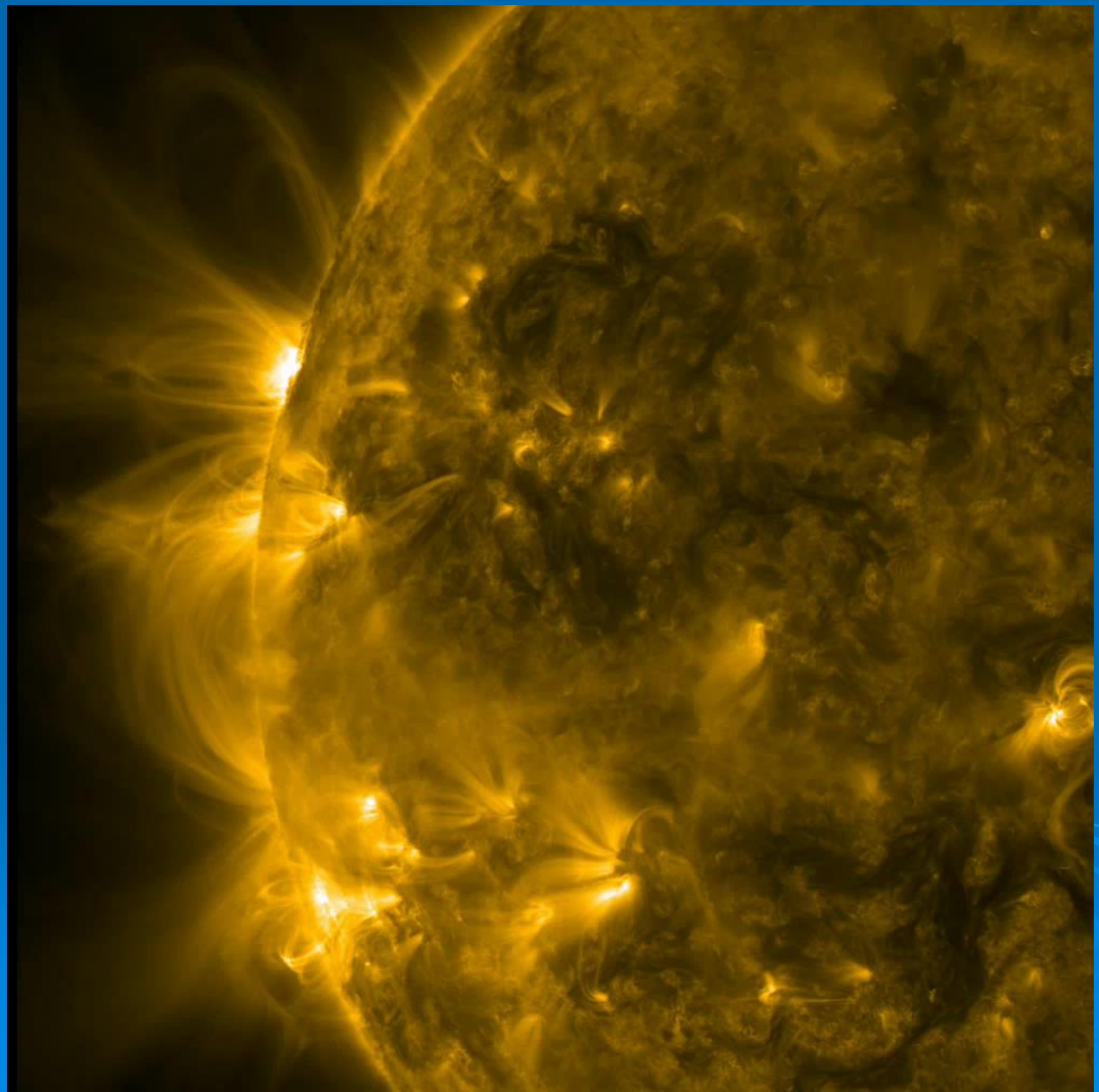

DNS in Two Forced Regions: Dynamo+NEMPI

S. Jabbari, A. Brandenburg, Dh. Mitra, N. Kleeorin and I. Rogachevskii, Astron. Astrophys., 459, 4046-4056 (2016).

All simulations are performed with the PENCIL CODE,

$$\rho\frac{\mathrm{D}\boldsymbol{U}}{\mathrm{D}t} = -c_{\mathrm{s}}^2\boldsymbol{\nabla}\rho + \boldsymbol{J}\times\boldsymbol{B} + \rho(\boldsymbol{f}+\boldsymbol{g}) + \boldsymbol{\nabla}\cdot(2\nu\rho\mathbf{S}),$$

$$\frac{\partial \boldsymbol{A}}{\partial t} = \boldsymbol{U}\times\boldsymbol{B} + \eta\nabla^2\boldsymbol{A},$$

$$\frac{\partial \rho}{\partial t} = -\boldsymbol{\nabla}\cdot\rho\boldsymbol{U},$$

Run	$\mathrm{Re_M}$	k_f/k_1	$z_\star/H_\rho$	$\lambda/\eta_{\mathrm{t0}}k_1^2$
D	16	30	-1	0.042
RM0	10	30	-1	0.05
RM1	**50**	**30**	**-1**	**0.014**
RM1zs	50	30	π	0.013
RM1k	50	5	-1	0.024
RM2	130	30	-1	0.005
RM3	260	30	-1	0.002
RM4	300	30	-1	0.001

$\frac{\rho_{bot}}{\rho_{top}} = 535;$ $\mathrm{Pm} = \frac{\nu}{\eta} = \frac{1}{2}$

$256^3; 512^3;$

FORCING:

1). White-in-time random forcing with the fractional helicity:

2). Helical forcing: $-\pi < z < z_0$ (bottom layer);

3). Non-helical forcing: $z_0 < z < \pi$ (upper layer).

$$\sigma(z-z_0) = \frac{\sigma_{\max}}{2}\left[1-\mathrm{erf}\left(\frac{z-z_0}{w_\mathrm{f}}\right)\right]$$

$\mathrm{Re} \equiv u_{\mathrm{rms}}/\nu k_\mathrm{f},$ $w_f = 0.08L_z$

BOUNDARY CONDITIONS:

1).The horizontal boundaries are periodic.

2). For the velocity we apply impenetrable, stress-free conditions.

3). For the magnetic field we use a) vertical field boundary conditions for z=L (at the top);
b) perfect conductor for z=0 (at the bottom) .

DNS in Two Forced Regions: Dynamo+NEMPI

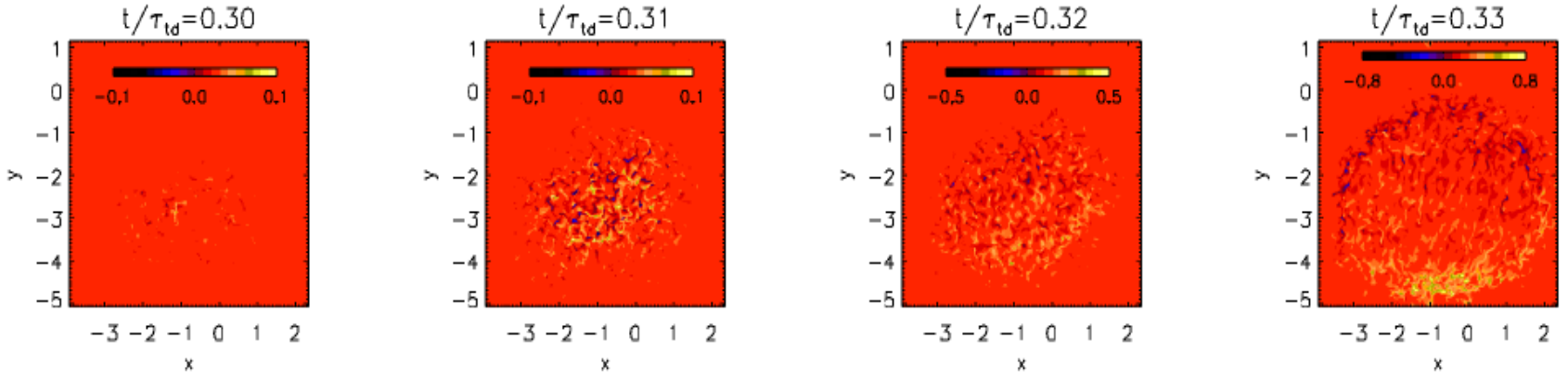

Figure 2. Vertical magnetic field at the top surface at different times (from $t/\tau_{\rm td} = 0.30$ to 0.33) from Run B. The magnetic field is normalized by $B^0_{\rm eq}$.

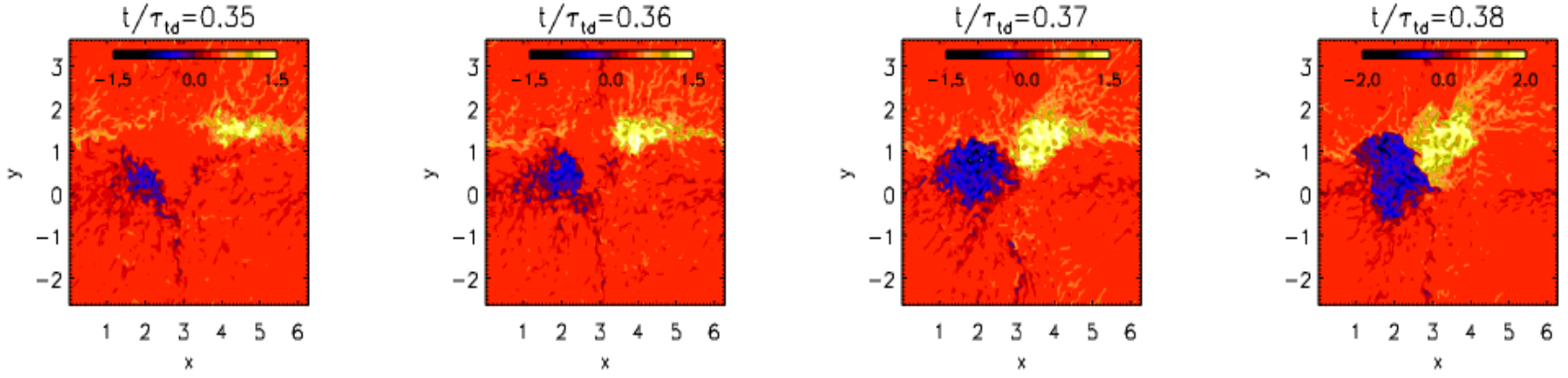

Figure 3. Same as Fig. 2, but at later times (from $t/\tau_{\rm td} = 0.35$ to 0.38) and the frame is re-centered, as illustrated in Fig. 4 below.

DNS in Two Forced Regions: Dynamo+NEMPI

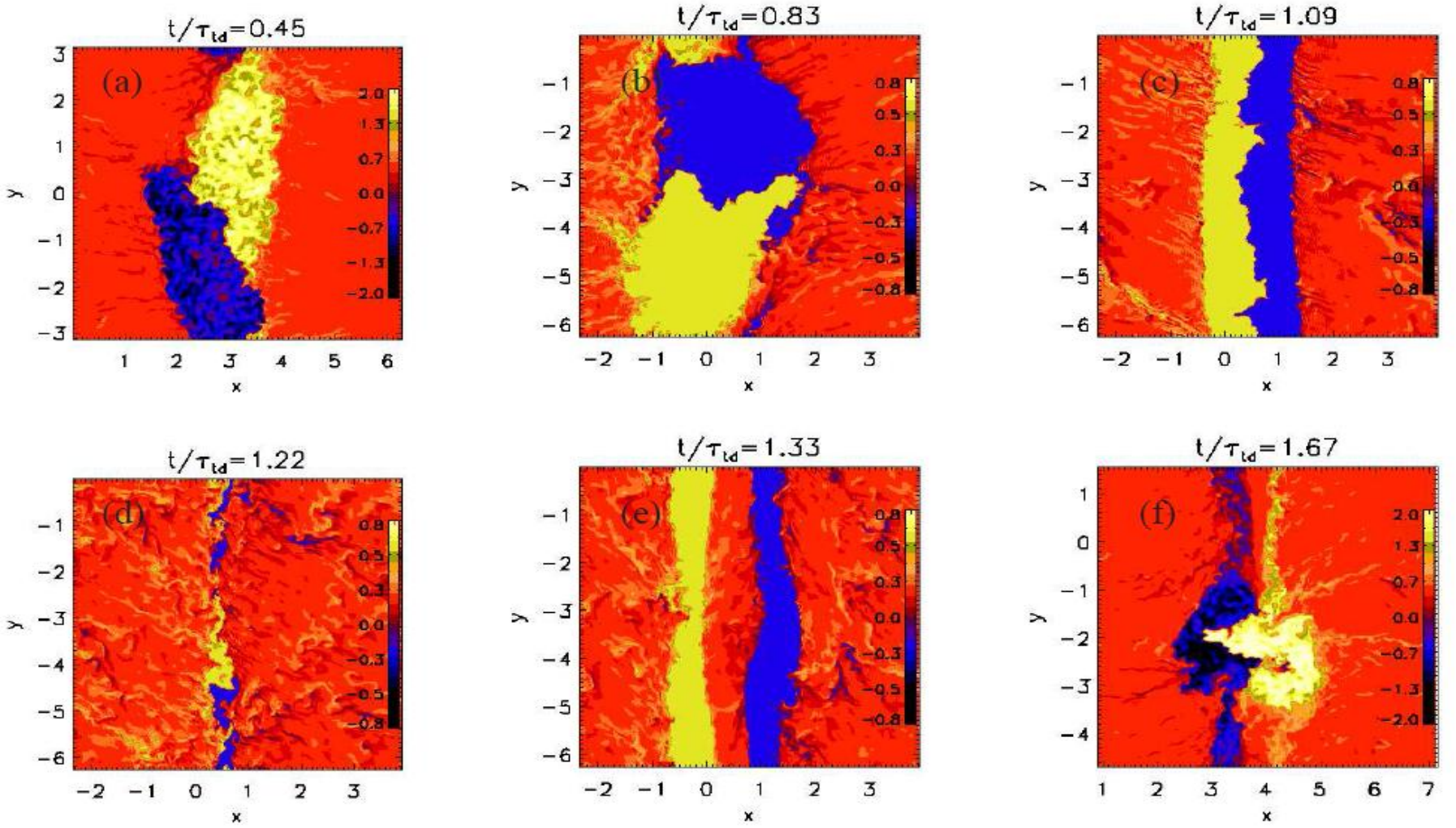

Figure 5. Evolution of the vertical magnetic field at the top surface. Snapshots at different times (from $t/\tau_{\rm td} = 0.45$ to $t/\tau_{\rm td} = 1.67$) are plotted.

DNS in Two Forced Regions: Reconnection

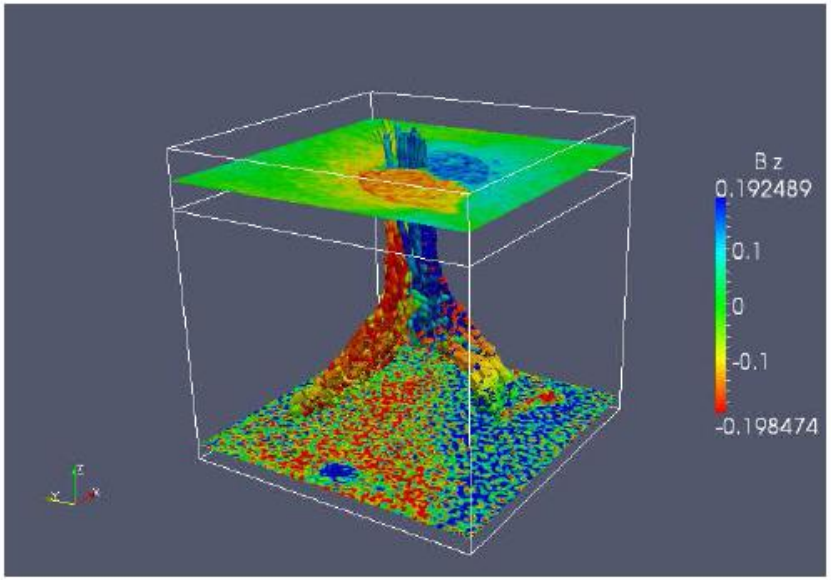

Figure 8. Magnetic field structure for Run A at time $t/\tau_{\rm td} \approx 1.2$. The z component of the magnetic field, B_z is plotted at $z/H_\rho = 3.$. The height up to which dynamo operates, $z_0/H_\rho = 2$, is also shown as a frame. Here magnetic field, B_z is not normalized, but in units of $\sqrt{\langle\rho(z=0)\rangle_{xy}}c_{\rm s}$. In the same units $B^0_{\rm eq} \approx 0.1$.

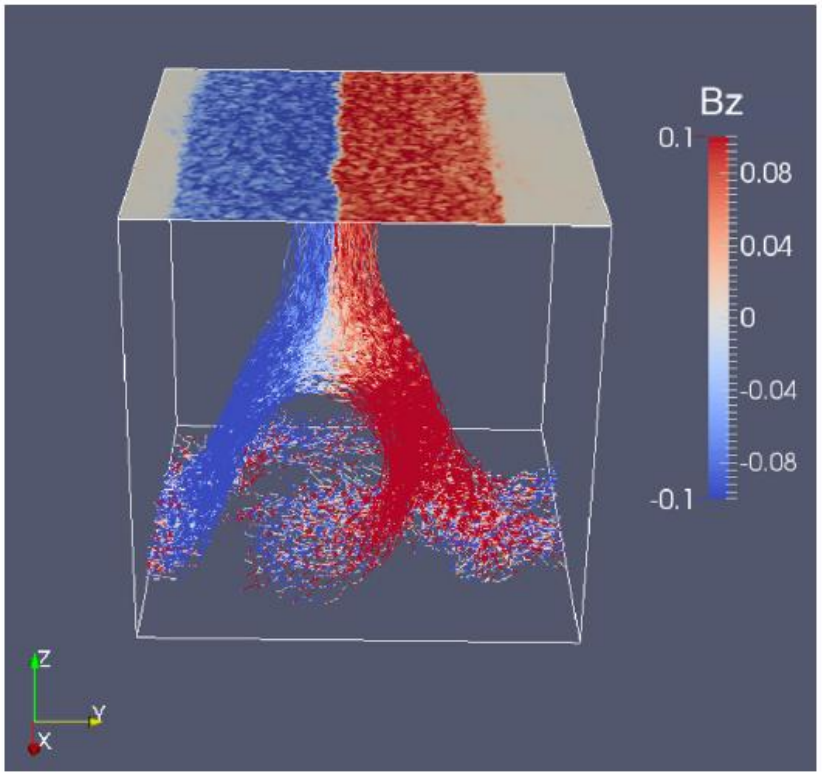

Figure 4. Three-dimensional visualization of vertical magnetic field, B_z at the surface (colour-coded) together with three-dimensional volume rendering of the vertical component of the magnetic field for Run RM1.

Reconnection Rate and Different Regimes

1. Sweet-Parker model (Parker (1957); Sweet (1969)):

$$V_{\rm rec} = V_{\rm A} S^{-1/2}$$

Lundquist number:

$$S = V_{\rm A} L/\eta$$

2. Lazarian-Vishniac (1999)

$$V_{\rm rec} \sim V_{\rm A} M_{\rm A}^2$$

Alfven Mach number:

$$M_{\rm A} = u_{\rm rms}/V_{\rm A}$$

3. Loureiro-Schekochihin-Cowley (2007)

$$V_{\rm rec} \sim 10^{-2} V_{\rm A}$$

Formation and Destruction of the Current Sheet

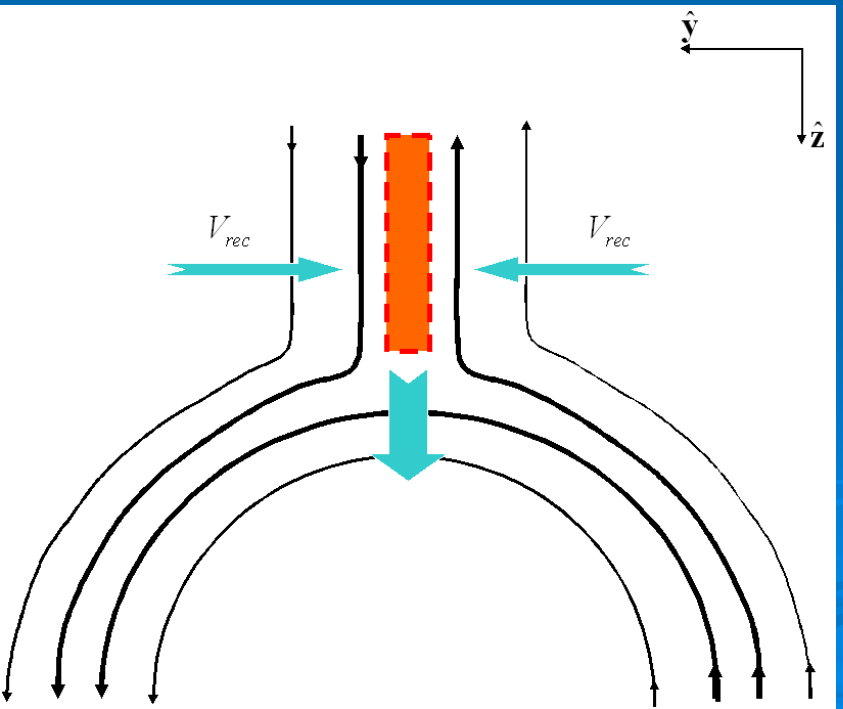

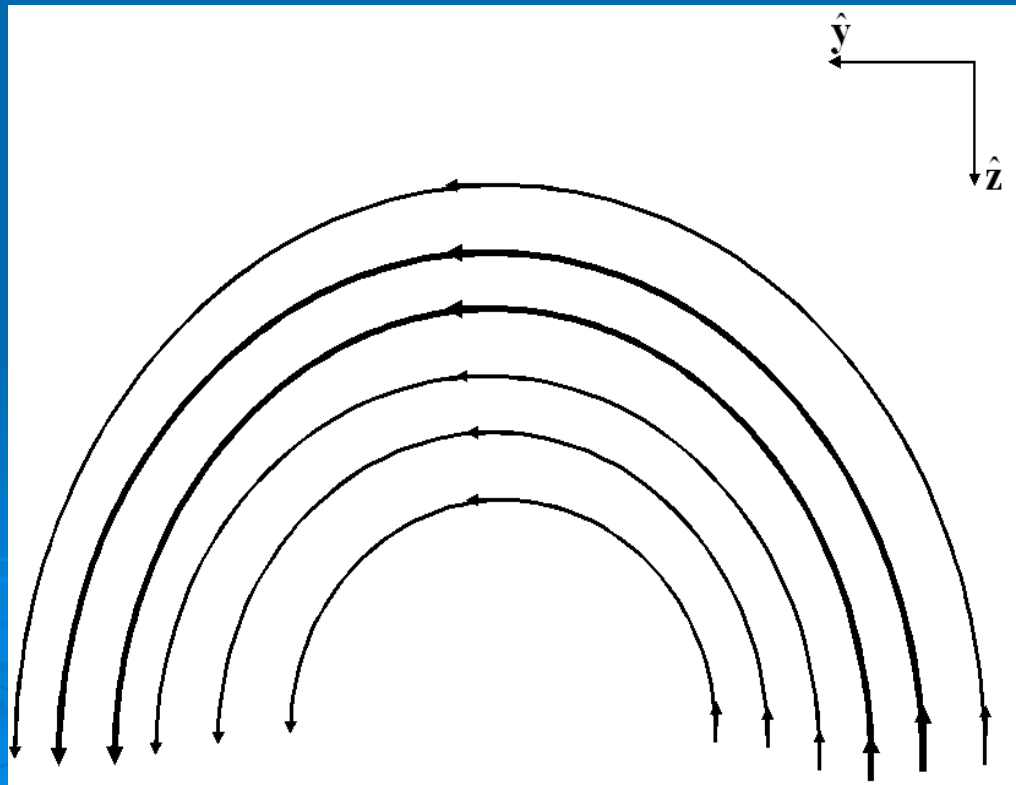

Formation of Current Sheet

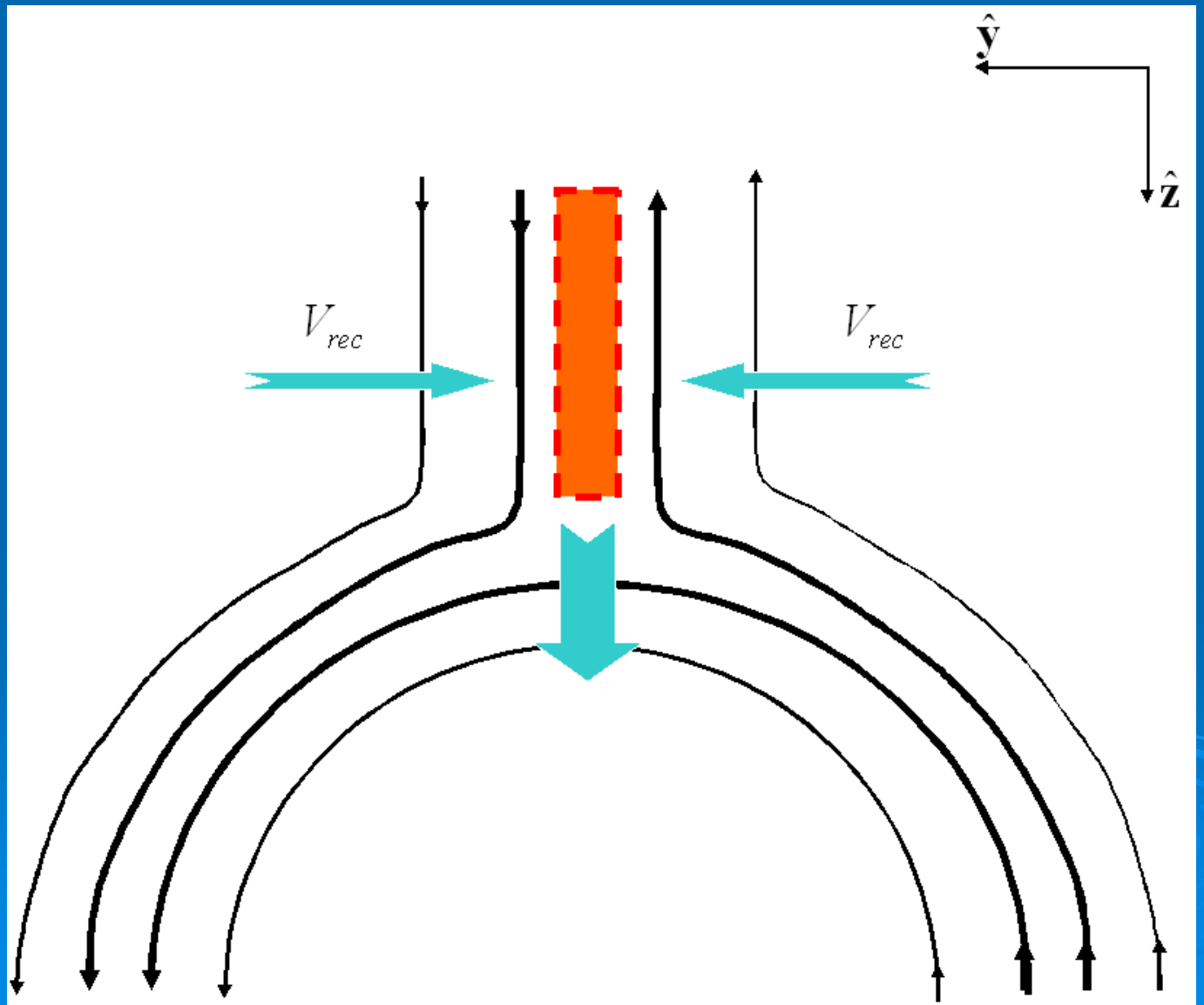

Formation of the Current Sheet and Reconnection

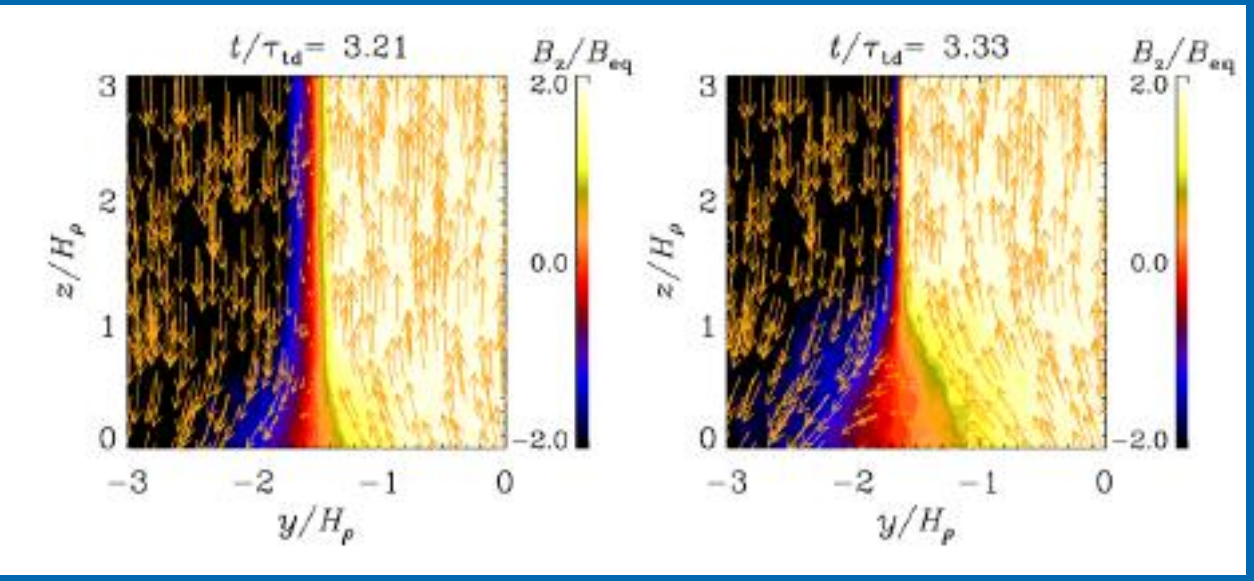

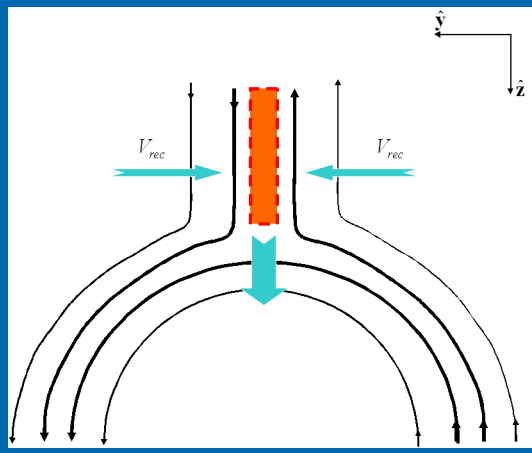

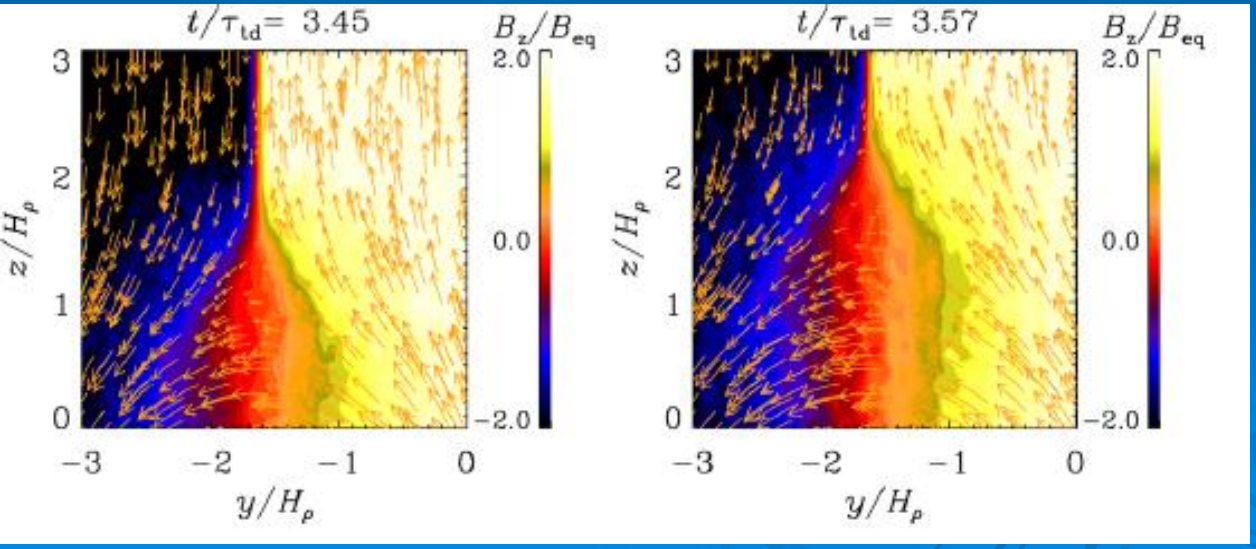

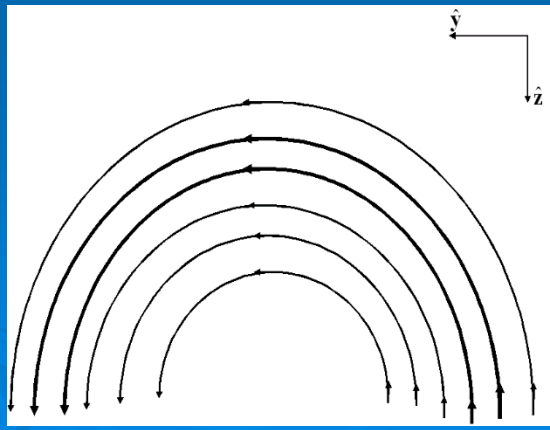

Reconnection Rate and Different Regimes

1. Sweet-Parker model (Parker (1957); Sweet (1969)):

$$V_{\rm rec} = V_{\rm A} S^{-1/2}$$

Lundquist number:

$$S = V_{\rm A} L/\eta$$

2. Lazarian-Vishniac (1999)

$$V_{\rm rec} \sim V_{\rm A} M_{\rm A}^2$$

Alfven Mach number:

$$M_{\rm A} = u_{\rm rms}/V_{\rm A}$$

3. Loureiro-Schekochihin-Cowley (2007)

$$V_{\rm rec} \sim 10^{-2} V_{\rm A}$$

Loureiro, N. F., Uzdensky, D. A., Schekochihin, A. A., Cowley, S. C., Yousef, T. A. 2009, MNRAS, 399, L146

Huang, Y.-M. & Bhattacharjee, A. 2010, Phys. Plasmas, 17, 062104

Formation of the Current Sheet and Reconnection

S. Jabbary, A. Brandenburg, Dh. Mitra, N. Kleeorin, I. Rogachevskii,
MNRAS 459, 4046 (2016).

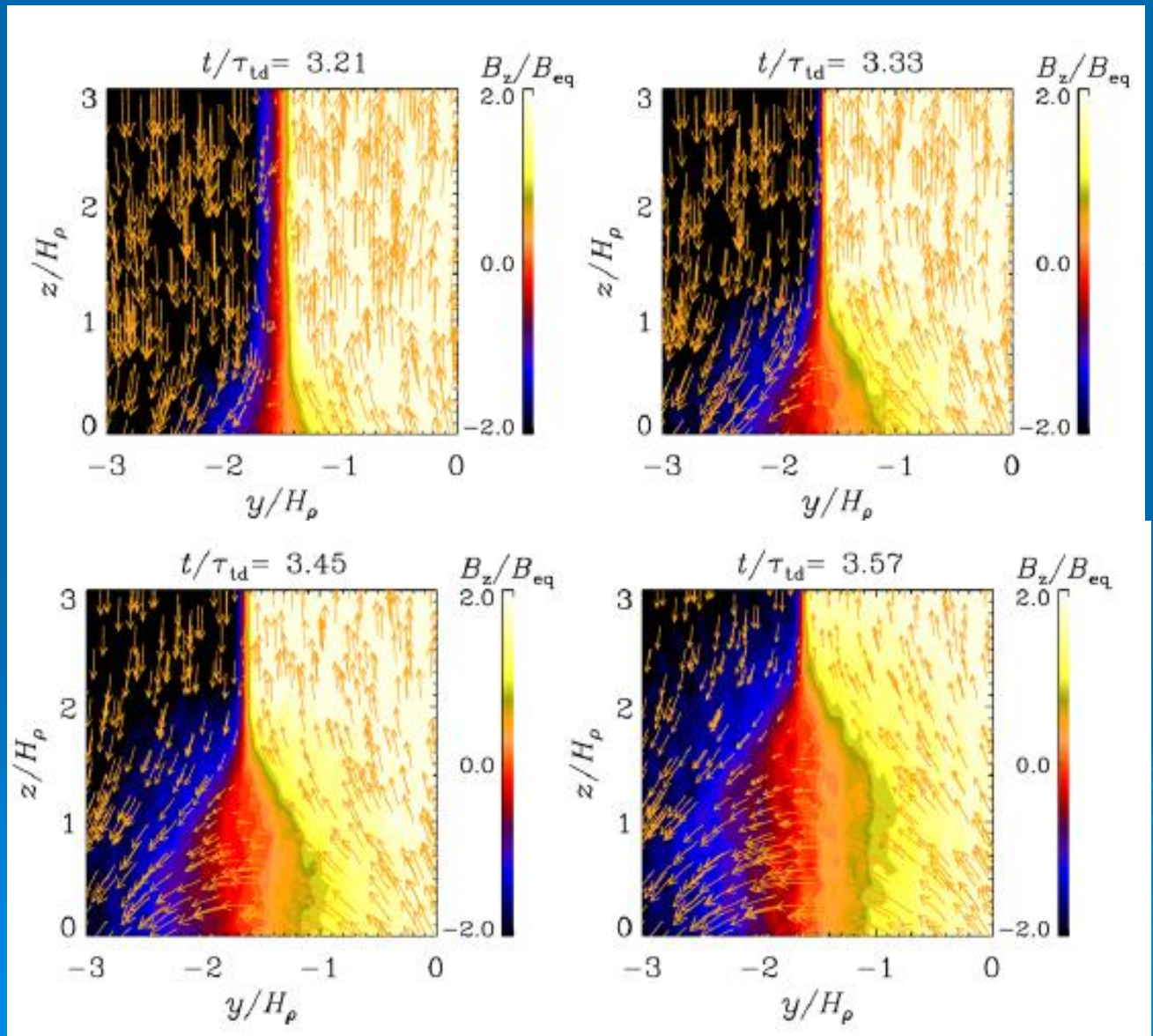

Reconnection Rate vs Lundqust Number

Loureiro-Schekochihin-Cowley (2007)

$$V_{\rm rec} \sim 10^{-2} V_{\rm A}$$

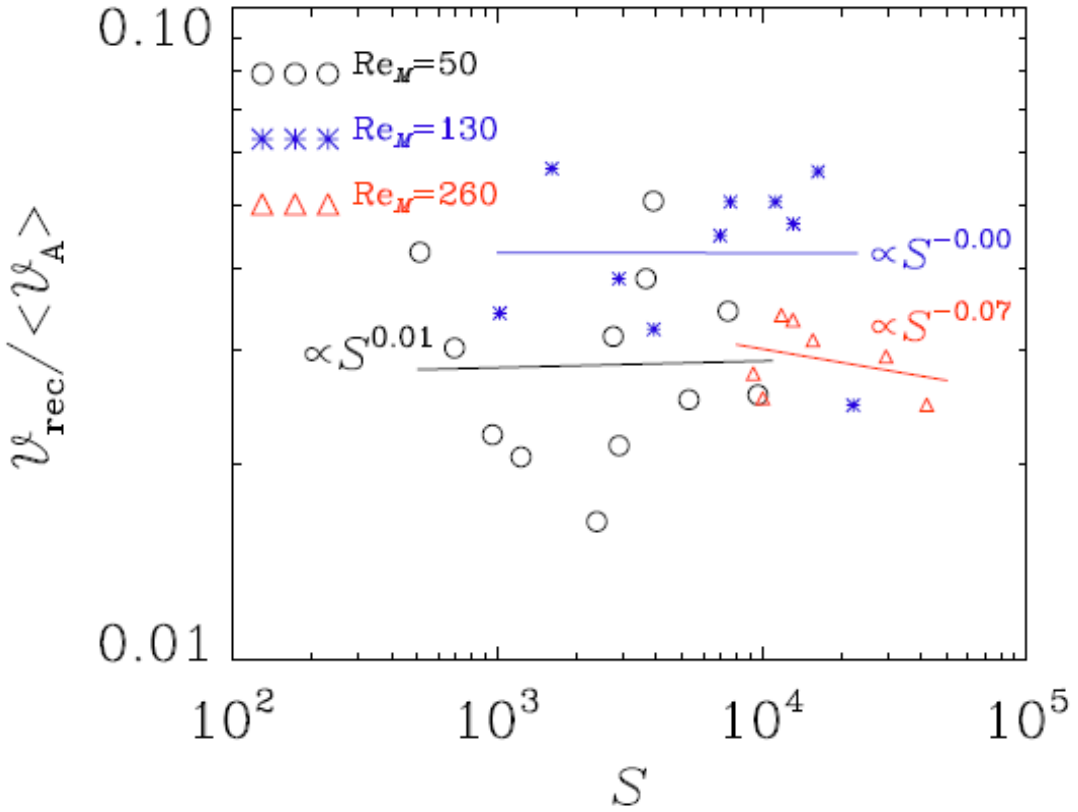

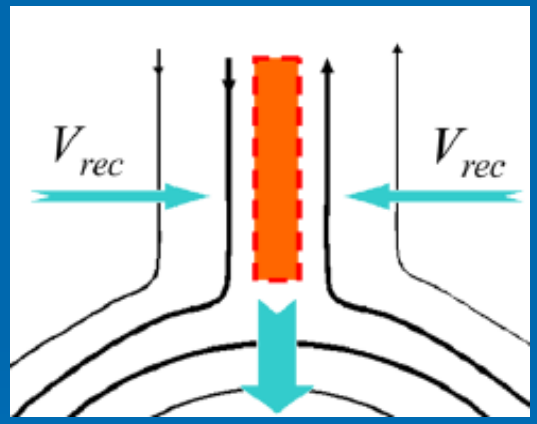

$$S = V_{\rm A} L/\eta$$

$$\mathrm{Re}_M = \frac{u_{\rm rms}}{\eta k_{\rm f}},\ \mathrm{Re} = \frac{u_{\rm rms}}{\nu k_{\rm f}},\ \mathrm{Pr}_M = \frac{\nu}{\eta},$$

Reconnection Rate vs Mach Number

Lazarian-Vishniac, ApJ 517, 700 (1999)

$$V_{\rm rec} \sim V_{\rm A} M_{\rm A}^2$$

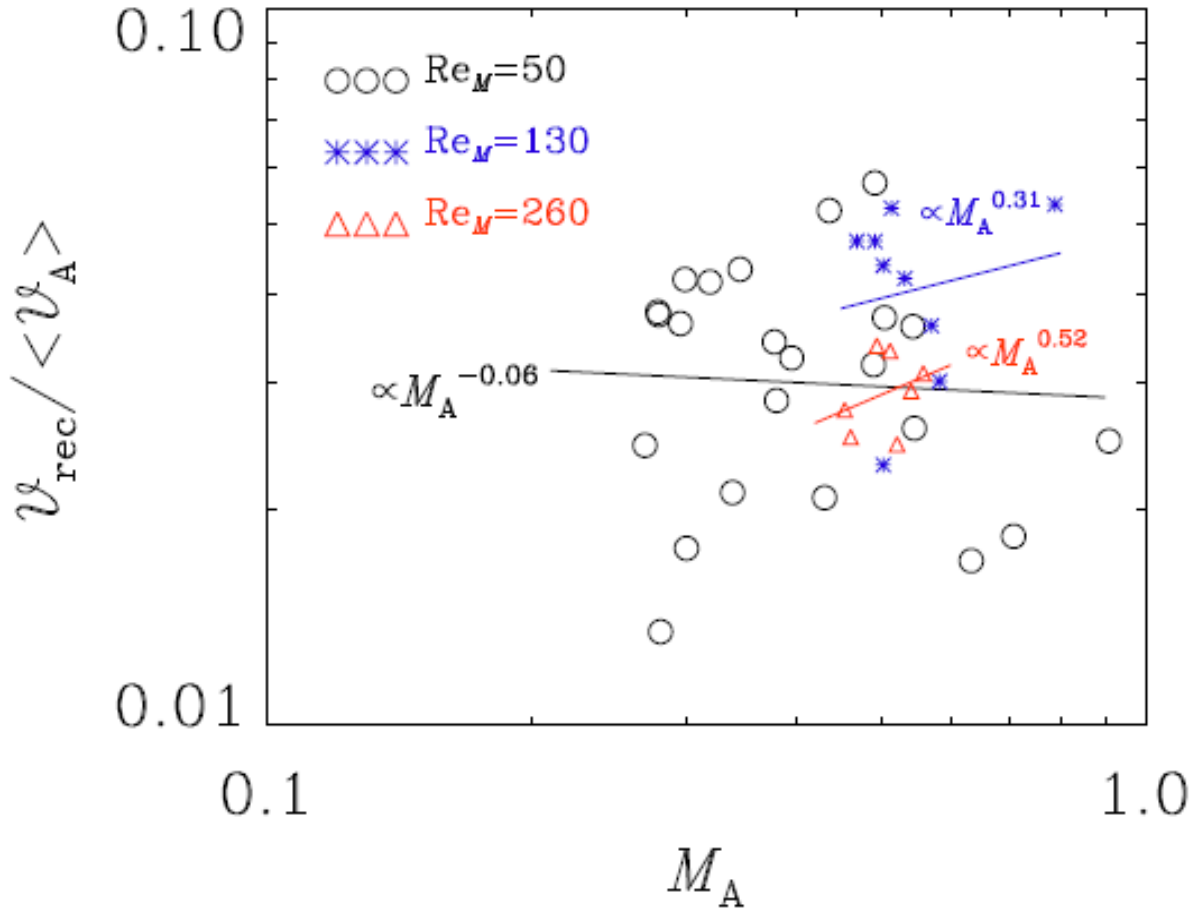

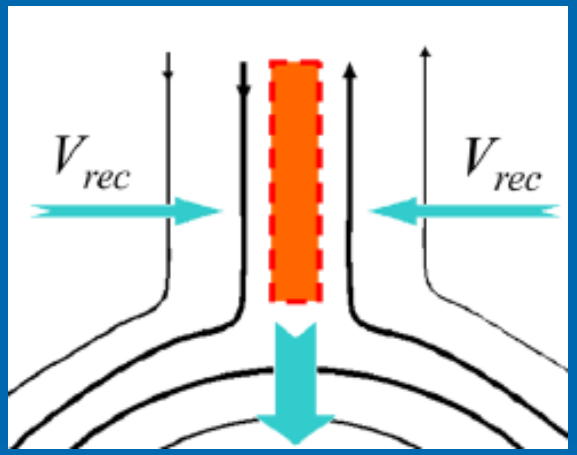

$$M_{\rm A} = u_{\rm rms}/V_{\rm A}$$

Active regions and Sunspots

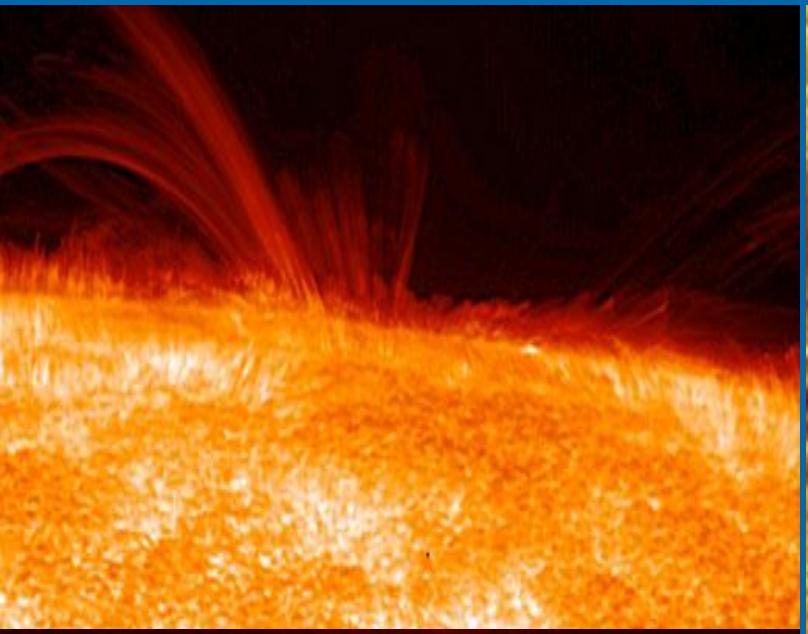

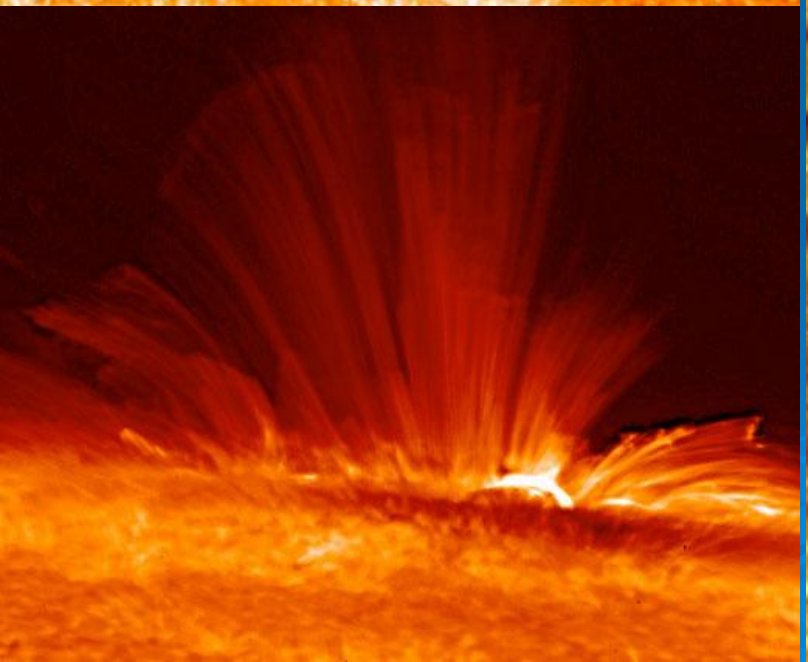

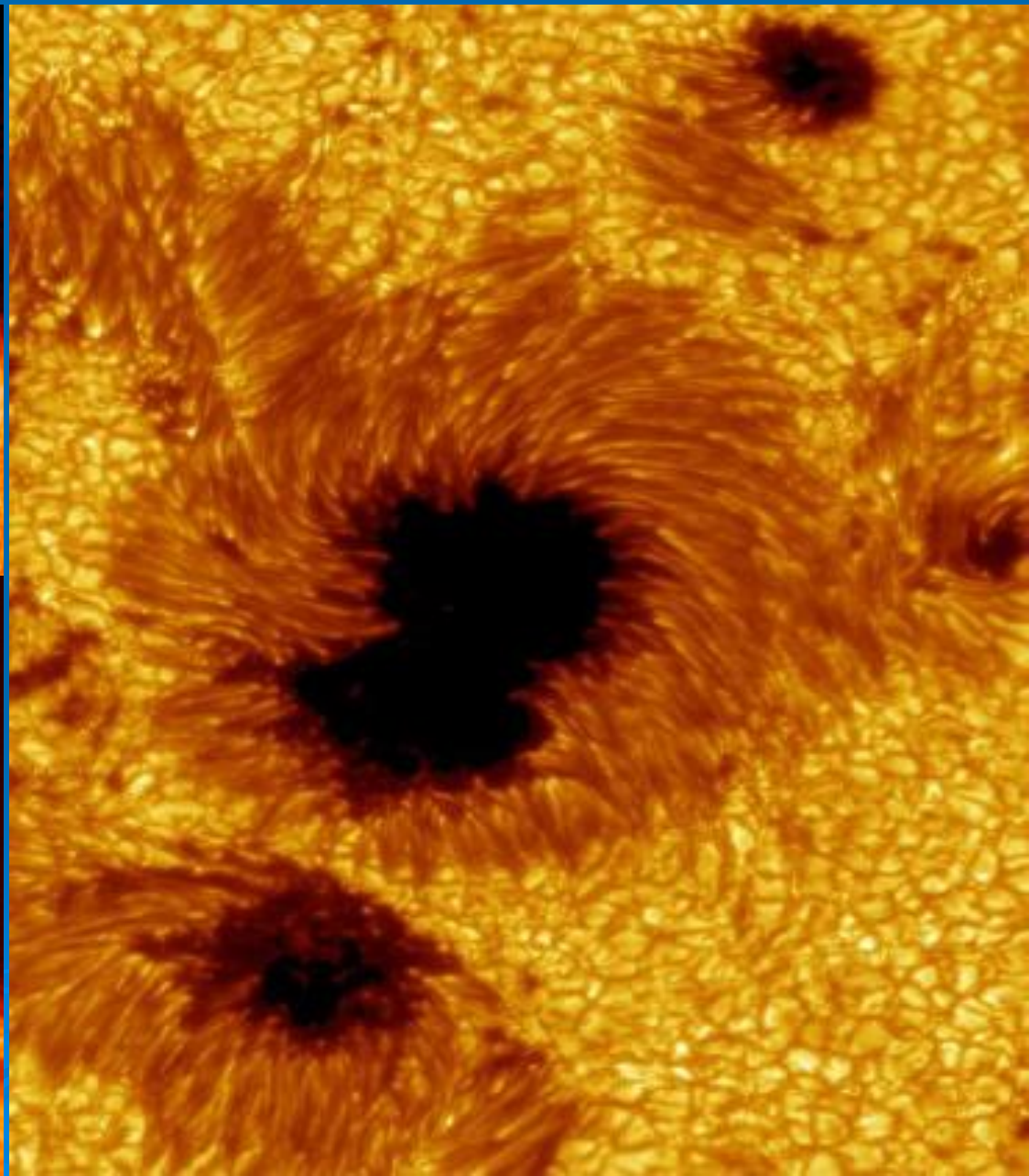

Theories of Magnetic Structure Formation

- 1. Interchange Instability (Magnetic Buoyancy Instability)
- 2. Negative Effective Magnetic Pressure Instability (NEMPI)

Magnetic Buoyancy Instability (Interchange Instability)

Let us estimate the growth rate of this instability. Neglecting dissipative processes for simplicity's sake, we shall retain only the Archimedes force in the momentum equation of the magnetic flux tube

$$\frac{d^2\zeta}{dt^2} = -\left(\frac{C_A}{C_s}\right)^2 \frac{gQ_p(L_B - L_\rho)}{L_B L_\rho}\zeta \ ,$$

where $C_A = \bar{B}_a/\sqrt{\mu\rho_a}$ is the Alfven velocity. The growth rate of this instability is given by

$$\gamma \simeq \frac{C_A}{L_\rho}\left[Q_p\left(\frac{L_\rho}{L_B} - 1\right)\right]^{1/2} \ .$$

Here $L_\rho \simeq C_s^2/g$.

For a weak turbulence ($Q_p \approx 1$), the small-scale turbulence will not affect large-scale processes. The criterion for instability due to buoyancy is $L_B < L_\rho$, and the instability is excited if the scale for change in the initial magnetic field is less than the density scale-height (Parker 1966).

Lorentz Force and Momentum Equation

$$\mathbf{J}\times\mathbf{B} = (\boldsymbol{\nabla}\times\mathbf{B})\times\mathbf{B} = -\boldsymbol{\nabla}\frac{\mathbf{B}^2}{2} + (\mathbf{B}\cdot\boldsymbol{\nabla})\mathbf{B} = -\nabla_j\left[\frac{1}{2}B^2\delta_{ij} - B_iB_j\right]$$

$$\frac{\partial}{\partial t}\rho\,\mathbf{U}_i = -\nabla_j\,\Pi_{ij}$$

where

$$\Pi_{ij} = \rho\,U_iU_j + \delta_{ij}\,(p + \frac{1}{2}\mathbf{B}^2) - B_iB_j - \sigma^{\nu}_{ij}(\mathbf{U}) + \ldots$$

Averaged equation: $\mathbf{U} = \bar{\mathbf{U}} + \mathbf{u}\,, \qquad \mathbf{B} = \bar{\mathbf{B}} + \mathbf{b}$

$$\frac{\partial}{\partial t}\bar{\rho}\,\bar{\mathbf{U}}_i = -\nabla_j\,\bar{\Pi}_{ij}$$

where

$$\bar{\Pi}_{ij} = \bar{\rho}\,\bar{U}_i\bar{U}_j + \delta_{ij}\,(\bar{p} + \frac{1}{2}\bar{\mathbf{B}}^2) - \bar{B}_i\bar{B}_j - \bar{\sigma}^{\nu}_{ij}(\bar{\mathbf{U}}) + \frac{1}{2}\langle\mathbf{b}^2\rangle\,\delta_{ij} - \langle b_ib_j\rangle + \bar{\rho}\langle u_iu_j\rangle + \ldots$$

3. Negative Effective Magnetic Pressure Instability (NEMPI)
(sum of turbulent and non-turbulent contributions)

$$\mathbf{J}\times\mathbf{B} = (\boldsymbol{\nabla}\times\mathbf{B})\times\mathbf{B} = -\boldsymbol{\nabla}\frac{\mathbf{B}^2}{2} + (\mathbf{B}\cdot\boldsymbol{\nabla})\mathbf{B} = -\nabla_j\left[\frac{1}{2}B^2\delta_{ij} - B_iB_j\right]$$

A. Brandenburg, K. Kemel, N. Kleeorin, I. Rogachevskii, Astrophys. J. 749, 179 (2012)

$$\mathcal{P}_{\rm eff}(\beta) = \tfrac{1}{2}[1 - q_{\rm p}(\beta)]\,\beta^2 \quad \text{versus} \quad \beta \equiv |\overline{\boldsymbol{B}}|/B_{\rm eq}$$

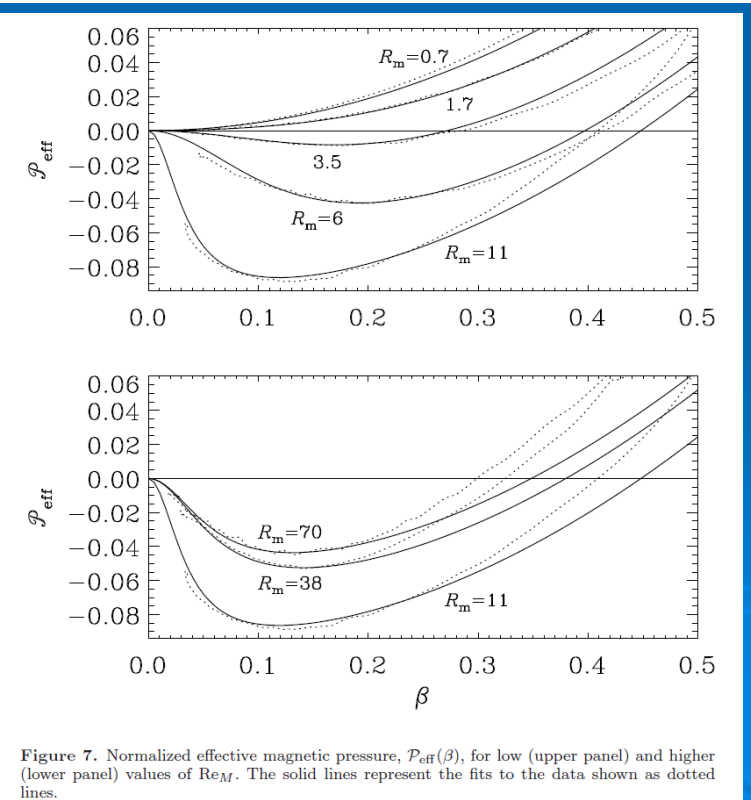

Figure 7. Normalized effective magnetic pressure, $\mathcal{P}_{\rm eff}(\beta)$, for low (upper panel) and higher (lower panel) values of Re_M. The solid lines represent the fits to the data shown as dotted lines.

$$\mathcal{P}_{\rm eff} = \frac{1}{2}(1 - q_p)\frac{\bar{\mathrm{B}}^2}{\mathrm{B}_{\rm eq}^2}$$

Effective magnetic pressure for Rm < 1 is positive, and for Rm > 1, it can be negative.

Quasi-linear theory works only for

$$\mathrm{Rm} \ll 1$$

Equation of State for Isotropic Turbulence

N. Kleeorin, I. Rogachevskii and A. Ruzmaikin, *Sov. Astron. Lett. 15, 274-277 (1989); Sov. Phys. JETP 70, 878-883 (1990)*

N. Kleeorin and I. Rogachevskii, *Phys. Rev. E 50, 2716-2730 (1994)*

I. Rogachevskii and N. Kleeorin, *Phys. Rev. E 76, 056307 (2007)*

The total turbulent pressure is reduced when magnetic fluctuations are generated

The equation of state for an isotropic turbulence

$$p_T = \frac{1}{3} W_m + \frac{2}{3} W_k \ ,$$

where p_T is the total (hydrodynamic plus magnetic) turbulent pressure,

$W_m = \langle \mathbf{b}^2 \rangle / 2\mu$ is the energy density of the magnetic fluctuations,

$W_k = \rho_0 \langle \mathbf{u}^2 \rangle / 2$ is the kinetic energy density.

Strong reduction of Turbulent Pressure

Combining the equations:

$$p_T = \frac{1}{3}W_m + \frac{2}{3}W_k = \frac{2}{3}(W_k + W_m) - \frac{1}{3}\mathrm{W_m}\,, \qquad \mathrm{W_k + W_m = const}\,,$$

we can express the change of turbulent pressure δp_T in terms of the change of the magnetic energy density δW_m

$$\delta \mathrm{p_T} = -\frac{1}{3}\delta \mathrm{W_m}$$

Therefore, the turbulent pressure is reduced when magnetic fluctuations are generated (i.e., $\delta \mathrm{W_m} > 0$).

Total Turbulent Energy

The total energy density W_T of the homogeneous turbulence with a nonzero uniform mean magnetic field is conserved

$$\mathrm{W_k + W_m = const.}$$

The uniform large-scale magnetic field performs no work on the turbulence. It can only redistribute the energy between hydrodynamic fluctuations and magnetic fluctuations.

The total energy density $\mathrm{W_T = W_k + W_m}$ of the homogeneous turbulence with a mean magnetic field $\bar{\mathrm{B}}$

$$\frac{\partial W_T}{\partial t} = I_T - \frac{W_T}{\tau_0} + \eta_T \frac{(\boldsymbol{\nabla} \times \bar{\mathrm{B}})^2}{\mu}$$

$I_T =$ is the energy source of turbulence,

W_T/τ_0 determines the dissipation of the turbulent energy.

Equation of State for Anisotropic Turbulence

The equation of state for an anisotropic turbulence

$$p_T = \frac{1}{3(1+\sigma/2)} W_m + \frac{2}{3}\left(\frac{1+3\sigma/4}{1+\sigma/2}\right) W_k \,,$$

where $0 \leq \sigma < \infty$ is the degree of anisotropy of turbulence. For a two-dimensional turbulence: $\sigma \to \infty$ and the equation of state reads:

$$p_T = \frac{2}{3\sigma} W_m + W_k = (W_k + W_m) - \mathbf{W_m} \,,$$

Thus, the change of turbulent pressure δp_T for the two-dimensional turbulence is

$$\delta \mathbf{p_T} = -\delta \mathbf{W_m}$$

Effective Magnetic Pressure

The total pressure is

$$p_{tot} = p_k + p_T + P_B(\bar{B}) \ ,$$

where p_k is the fluid pressure and $P_B(\bar{B}) = \frac{\bar{\mathrm{B}}^2}{2\mu}$ is the magnetic pressure of the mean field.

Now we examine the part in p_{tot} that depends on the mean (large-scale) magnetic field $\bar{\mathrm{B}}$:

$$\mathrm{P_m(\bar{B})} = P_B(\bar{B}) - \mathrm{q_p(\bar{B})}\frac{\bar{\mathrm{B}}^2}{2\mu} = (1 - \mathrm{q_p(\bar{B})})\frac{\bar{\mathrm{B}}^2}{2\mu} \equiv Q_p(\bar{B})\frac{\bar{\mathrm{B}}^2}{2\mu} \ ,$$

$$p_{\mathrm{tot}} = p + \mathrm{P_m(\bar{B})} = p + \mathrm{Q_p(\bar{B})}\frac{\bar{\mathrm{B}}^2}{2\mu} \ ,$$

where $p = p_k + p_T^{(0)}$. The pressure $P_m(\bar{B})$ is the combined mean magnetic pressure.

DNS: The Result is Robust

$$\mathcal{P}_{\rm eff} = \frac{1}{2}(1-q_p)\frac{\bar{\rm B}^2}{\rm B_{eq}^2}$$

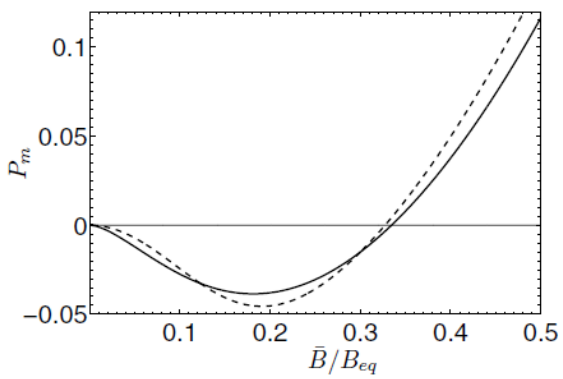

Fig. 3 The effective mean magnetic pressure $P_m(\overline{B}) = (1 - q_{\rm p})\overline{B}^2/\overline{B}_{\rm p}^2$ determined by Rogachevskii & Kleeorin (2007) – solid line, and by the model described by Eq. (26) – dashed line ($\overline{B}_{\rm p} = 0.21\, c_{\rm s0}\rho_0^{1/2}$ and $q_{\rm p0} = 4$).

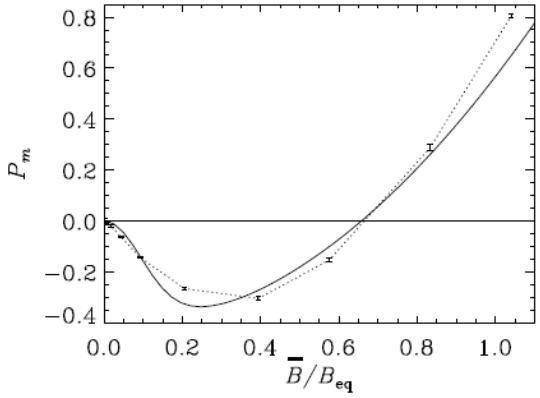

Fig. 4 Same as Fig. 3, but from simulation (dotted line). The solid line shows a fit [Eq. (26)] with $\overline{B}_{\rm p} = 0.022\, c_{\rm s0}\rho_0^{1/2}$ (corresponding to $\overline{B}_{\rm p}/B_{\rm eq} = 0.18$) and $q_{\rm p0} = 21$.

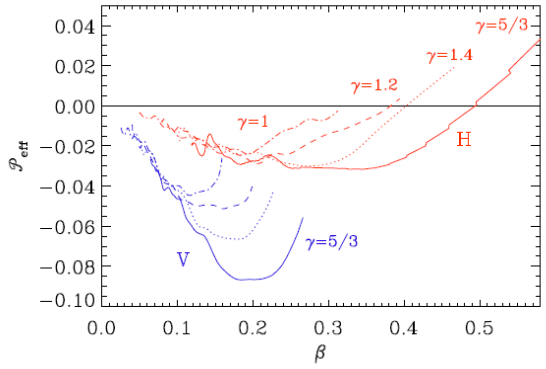

Fig. 7. Effective magnetic pressure obtained from DNS in a polytropic layer with different γ for horizontal (H, red curves) and vertical (V, blue curves) mean magnetic fields.

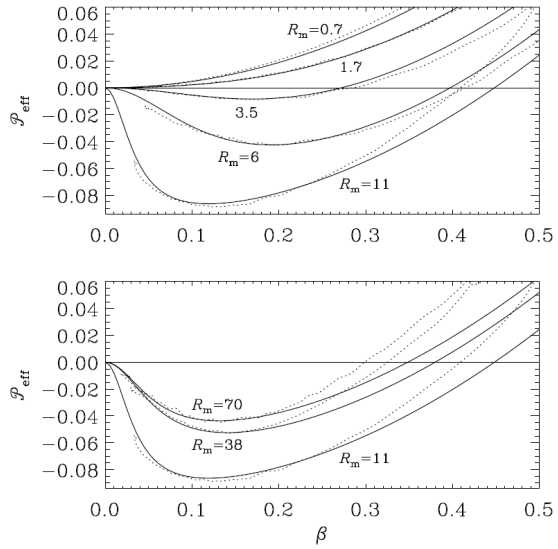

Figure 7. Normalized effective magnetic pressure, $\mathcal{P}_{\rm eff}(\beta)$, for low (upper panel) and higher (lower panel) values of Re_M. The solid lines represent the fits to the data shown as dotted lines.

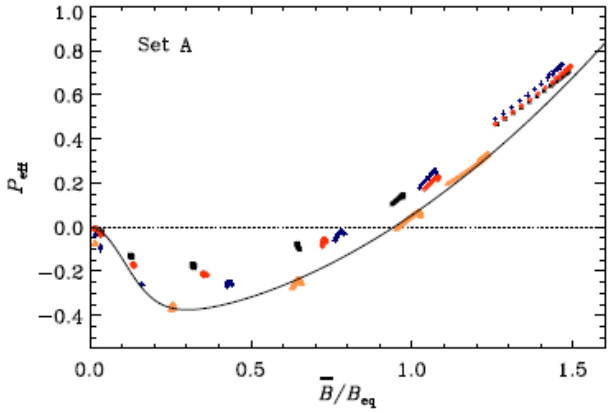

Figure 2. Effective magnetic pressure as a function of the mean magnetic field from weakly stratified Runs A1–A29 with an imposed horizontal field $\boldsymbol{B}_0 = B_0\hat{\boldsymbol{x}}$. The black stars, red diamonds, blue crosses, and yellow triangles denote simulations with Rm $\approx$ 10, 20, 50, and 70, respectively. We omit points near the boundaries at $z/d < 0.35$ and $z/d > 0.65$. The dashed and dotted lines correspond to approximate fits determined by Eq. (30), with $q_{p0} = 35$ and $B_p = 0.2B_{\rm eq}$, respectively.

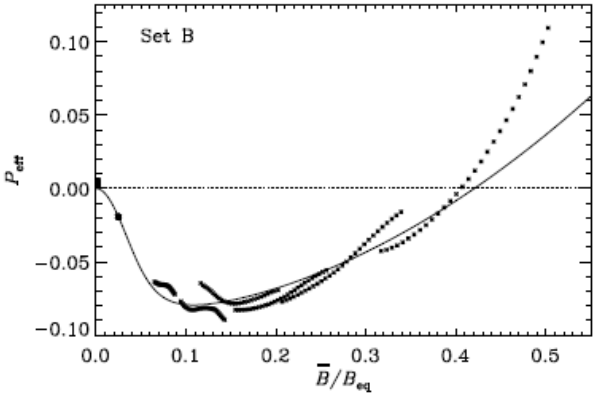

Figure 3. Same as Figure 2 but for Runs B1–B8 for Rm = 40–50. The solid line corresponds to a fit with $q_{p0} = 70$ and $B_p = 0.063B_{\rm eq}$

Methods and Approximations

- **Quasi-Linear Approach** or Second-Order Correlation Approximation (SOCA) or First-Order Smoothing Approximation (FOSA); **Rm << 1 , Re << 1**

N. Kleeorin, I. Rogachevskii and A. Ruzmaikin, *Sov. Phys. JETP 70, 878-883 (1990)*
A. Brandenburg, K. Kemel, N. Kleeorin, I. Rogachevskii, Astrophys. J. 749, 179 (2012)

- **Tau-approaches** (spectral tau-approximation) – **third-order or high-order closure; Re >> 1 and Rm >> 1**

N. Kleeorin, I. Rogachevskii and A. Ruzmaikin, *Sov. Phys. JETP 70, 878-883 (1990)*
I. Rogachevskii and N. Kleeorin, *Phys. Rev. E 76, 056307 (2007)*

- **Renormalization Procedure** (renormalization of turbulent transport coefficients) - **Re >> 1 and Rm >> 1, there is no separation of scales.**

N. Kleeorin and I. Rogachevskii, *Phys. Rev. E 50, 2716-2730 (1994)*

Large-Scale MHD-Instability (NEMPI)

A. Brandenburg, K. Kemel, N. Kleeorin, Dh. Mitra, and I. Rogachevskii,
Astrophys. J. Lett. 740, L50 (2011); Solar Phys. 280, 321-333 (2012).

$$\mathcal{P}_{\rm eff} = \frac{1}{2}(1-q_p)\frac{\bar{\rm B}^2}{{\rm B}_{\rm eq}^2}$$

$$\lambda = \frac{v_{\rm A}}{H_\rho}\left(-2\frac{{\rm d}\mathcal{P}_{\rm eff}}{{\rm d}\beta^2}\right)^{1/2}\frac{k_x}{k}.$$

Slow growth

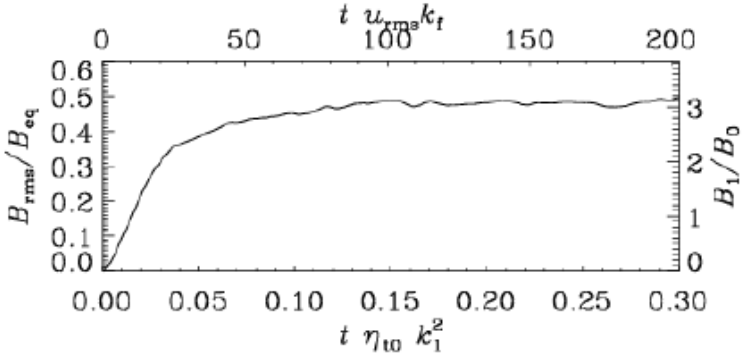

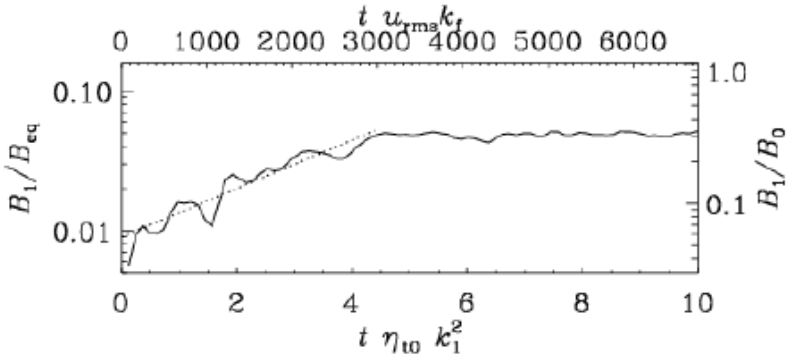

- Several thousand turnover times
- Or ½ a turbulent diffusive time
- Exponential growth → linear instability of an already turbulent state

Time-evolution of the Magnetic Spot

A. Brandenburg, N. Kleeorin and I. Rogachevskii, Astrophys. J. Lett., 776, L23 (2013)

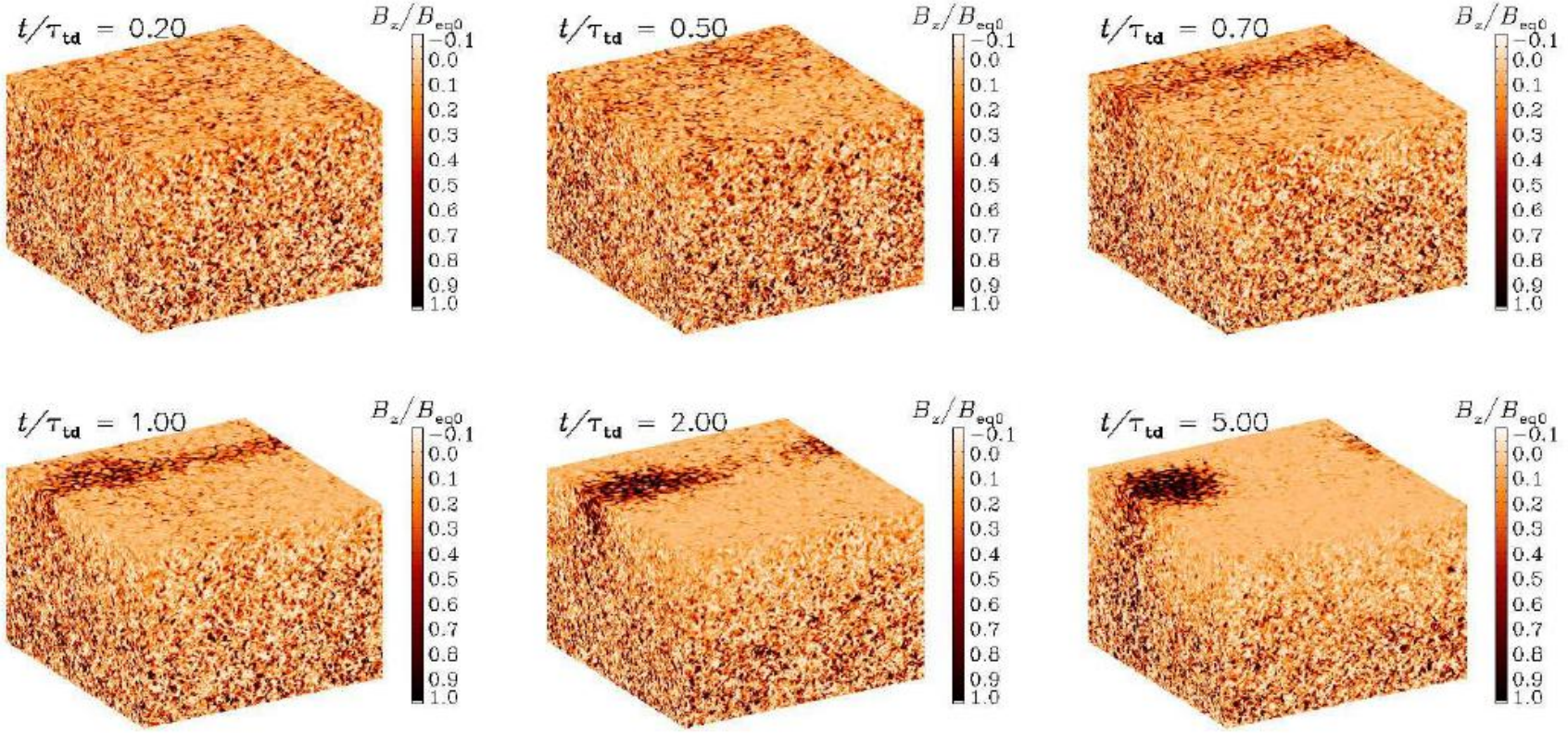

FIG. 1.— Evolution from a statistically uniform initial state toward a single spot for $B_{z0}/B_{eq0} = 0.02$. Here, B_z/B_{eq0} is shown on the periphery of the domain. Dark shades correspond to strong vertical fields. Time is in units of τ_{td}.

$\mathrm{Pr}_M = 0.06 - 1$

Formation and Destruction of Bipolar Magnetic Structures

J. Warnecke, I.R. Losada, A. Brandenburg, N. Kleeorin and I. Rogachevskii,
Astrophys. J. Lett., 777, L37 (2013); Astron. Astrophys., 589, A125 (2016).

Imposed horizontal field.

$k_f = 30\, k_1;$

512 x 512 x 1024; 1024^3

BOUNDARY CONDITIONS at the top and bottom:

$U_z = 0, \quad \nabla_z U_x = \nabla_z U_y = 0$

But

$z = -\pi$:

$B_z = 0, \quad \nabla_z B_x = \nabla_z B_y = 0$

$z = 2\pi$:

$B_x = B_y = 0.$

Re=40, $\mathrm{Pr}_M = 0.06 - 1$

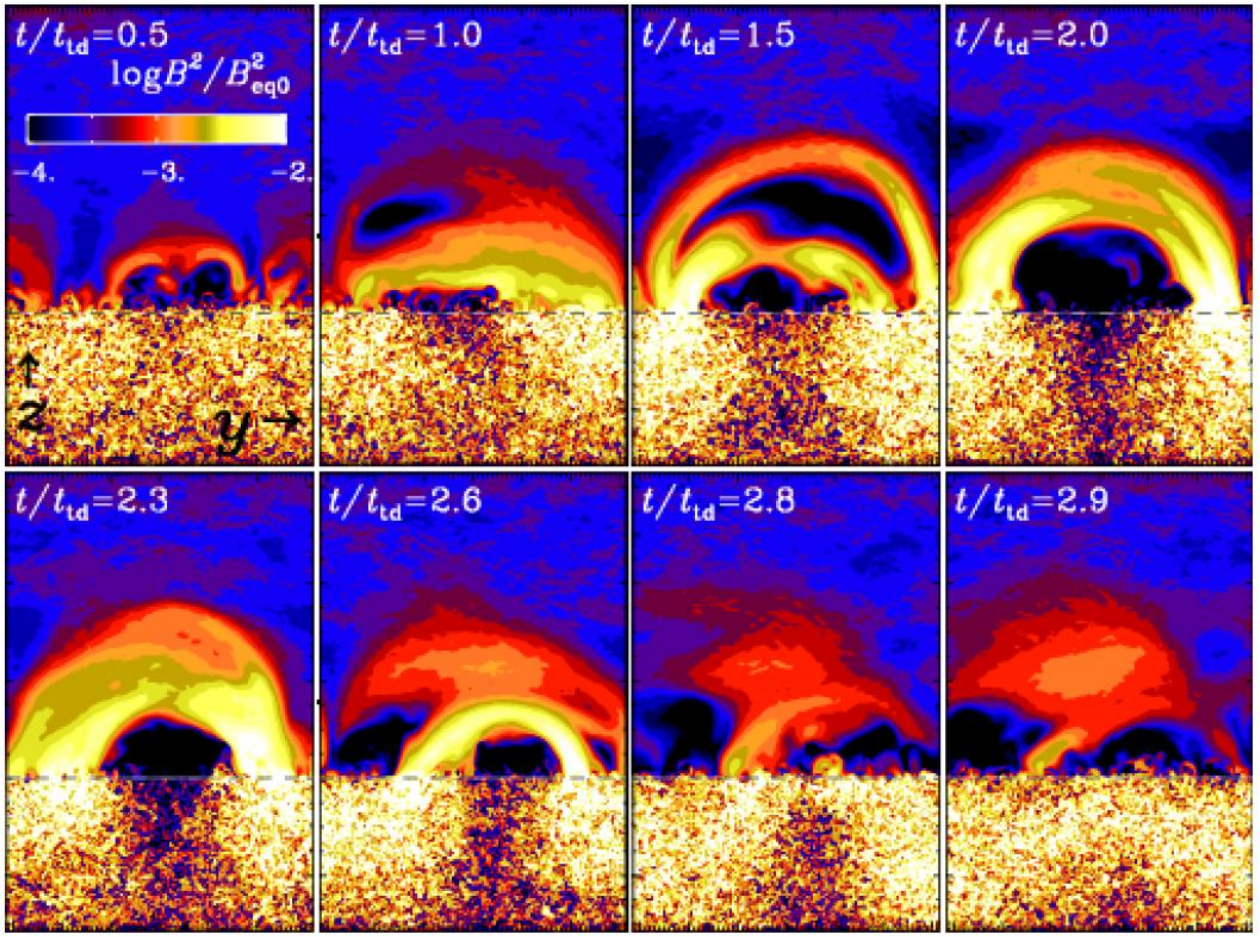

FIG. 5.— Time series of B^2/B^2_{eq0} in a vertical cut through the bipolar region at $x = 0$. Note the y axis is shifted the see the formation of the loop.

Formation and Destruction of Bipolar Magnetic Structures

J. Warnecke, I.R. Losada, A. Brandenburg, N. Kleeorin and I. Rogachevskii,
Astrophys. J. Lett., 777, L37 (2013); Astron. Astrophys., 589, A125 (2016).

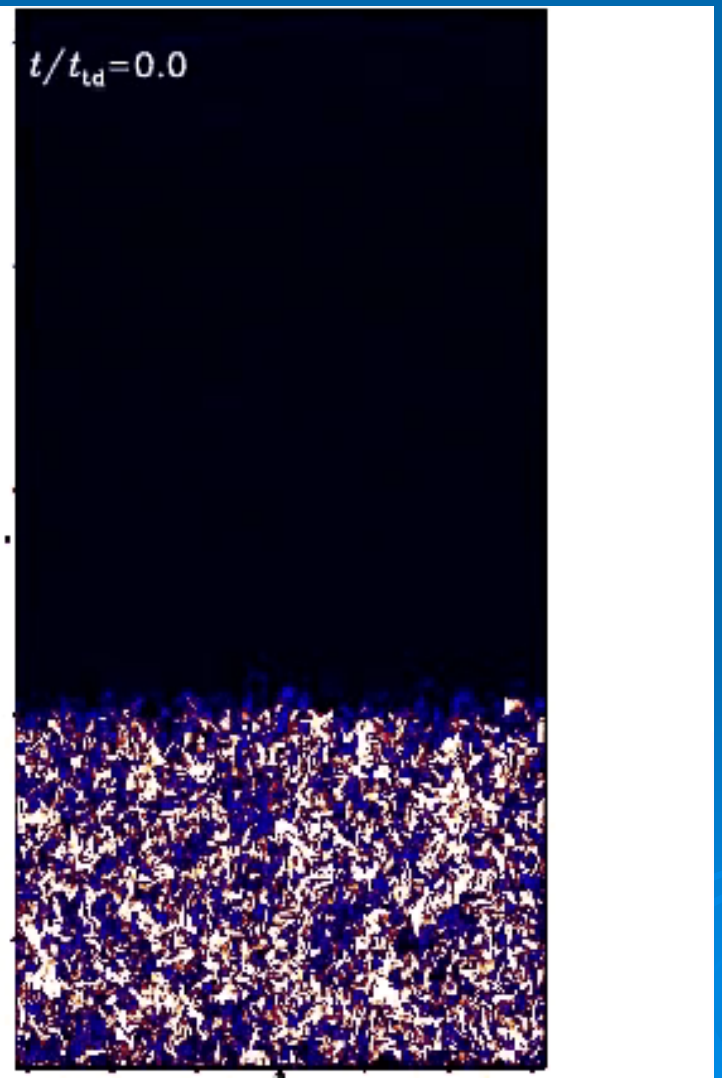

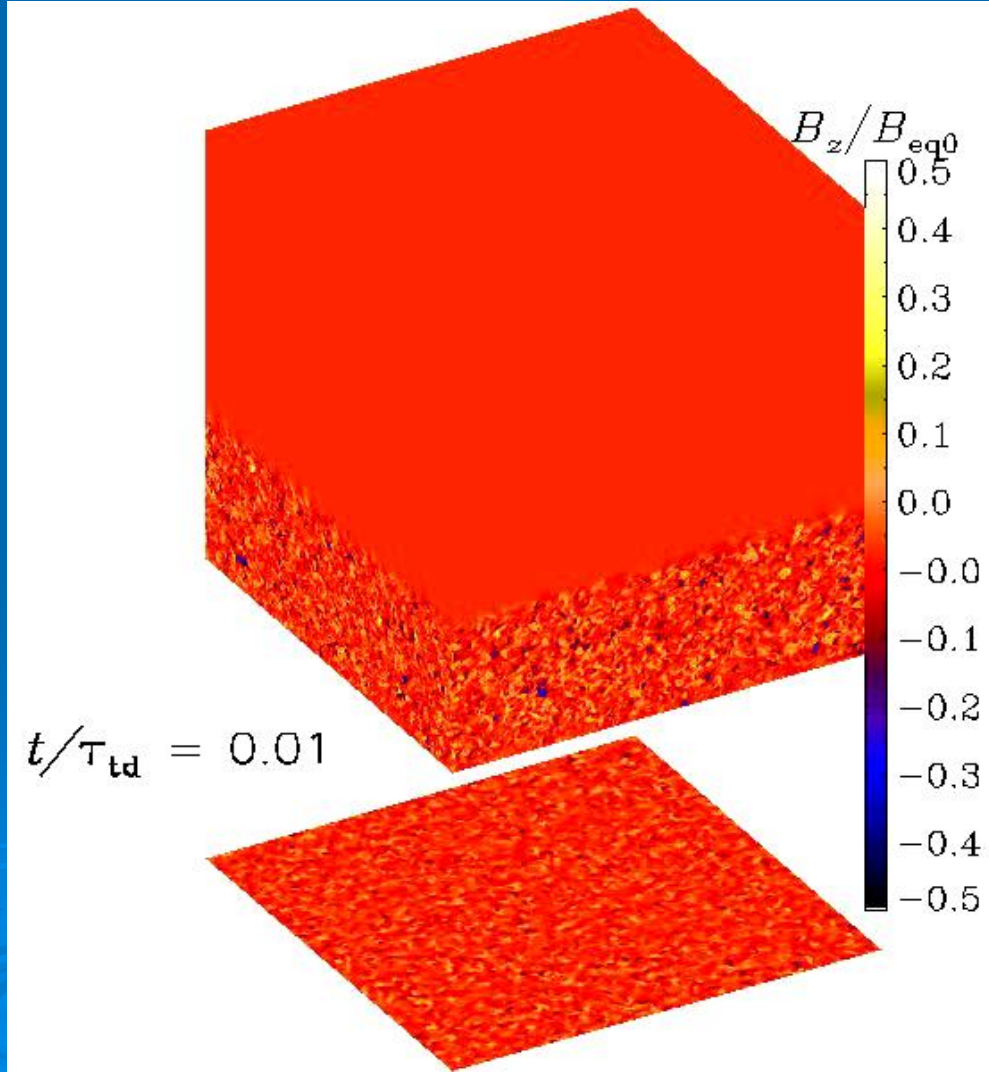

Magnetic Structures

J. Warnecke, I.R. Losada, A. Brandenburg, N. Kleeorin and I. Rogachevskii, Astrophys. J. Lett., 777, L37 (2013), Astron. Astrophys., 589, A125 (2016).

Simulations

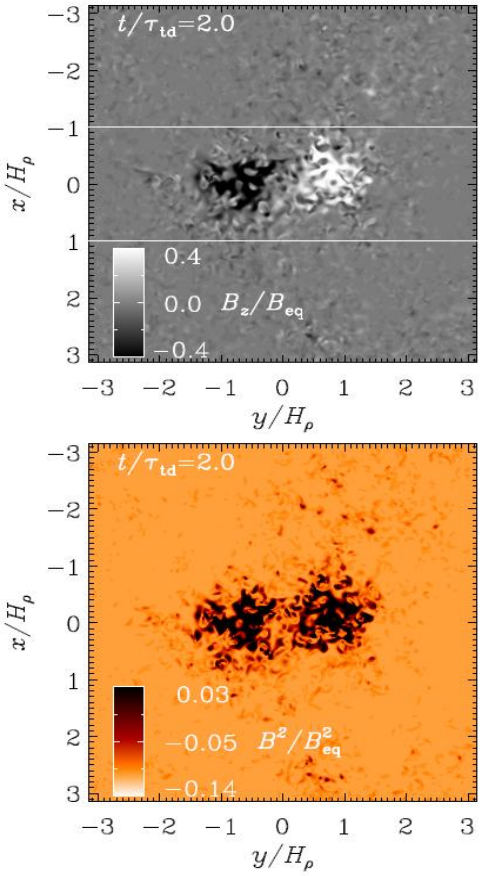

FIG. 1.— *Upper panel:* normalized vertical magnetic field B_z/B_{eq} of the bipolar region at the surface ($z = 0$) of the simulation domain. The white lines delineate the area shown in Figure 3. *Lower panel:* normalized magnetic energy B^2/B_{eq}^2 of the two regions relative to the rest of the surface. Note that we clip both color tables to increase the visualization of the structure. The field strength reaches around $B_z/B_{eq} = 1.4$.

Sunspots

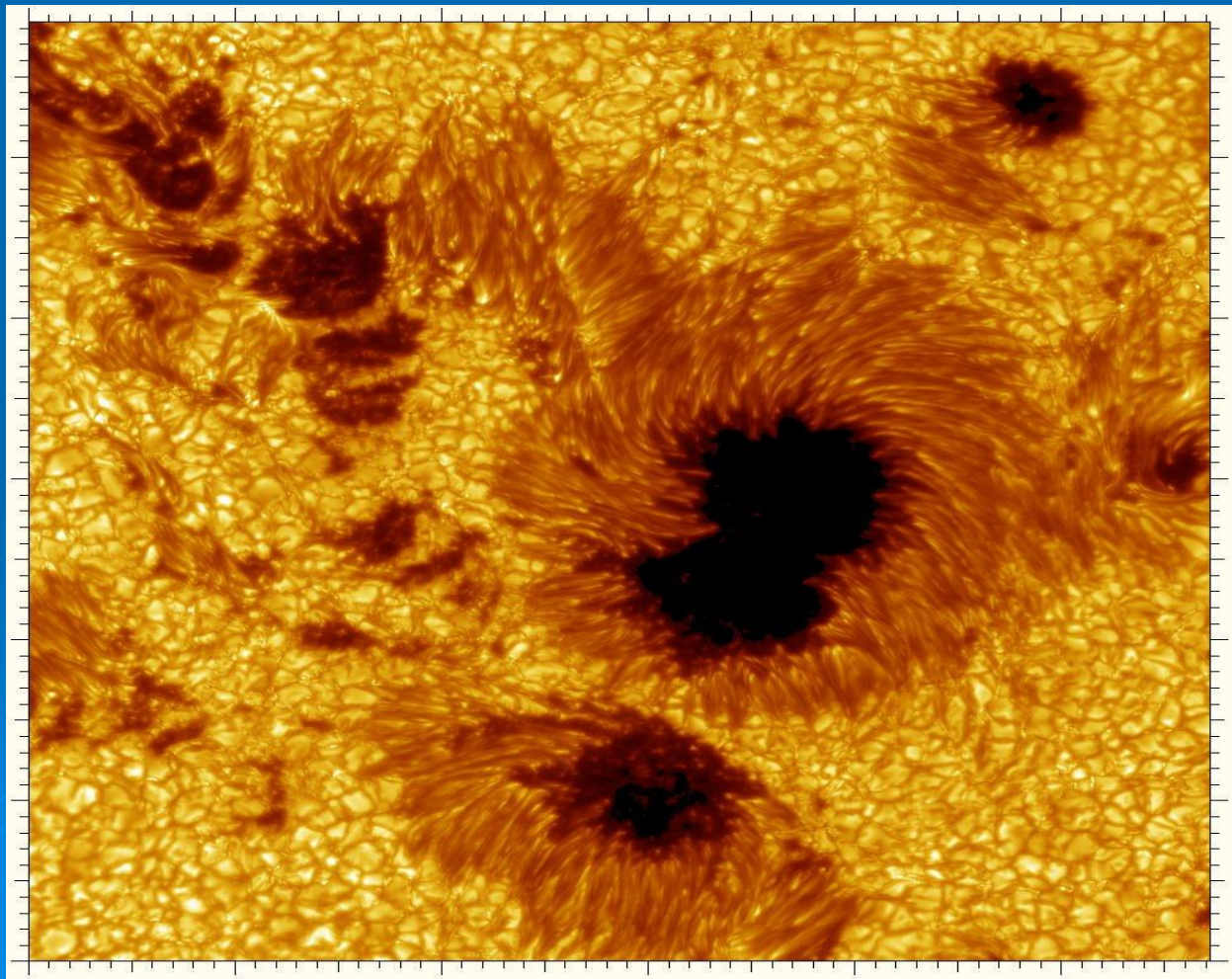

Summary

- Generation of magnetic fluctuations in a turbulence with large plasma beta results in a strong reduction of the large-scale magnetic pressure, so that effective magnetic pressure (sum of turbulent and non-turbulent contributions) can be negative.
- This causes excitation of negative effective magnetic pressure instability (NEMPI) and formation of the large-scale bipolar magnetic structures which are reminiscent Active Regions.
- DNS of two-layer systems with a helical forcing layer demonstrate formation of bipolar structures and turbulent reconnection with the rate that is independent of magnetic resistivity and Lundquist number. This is the first example of turbulent reconnection in nonlinear dynamos.

THE END